ELSEVIER

Polymer 40 (1999) 6991–7012

polymer

# A mechanistic model of case II diffusion of a diluent into a glassy polymer

A.S. Argon*, R.E. Cohen, A.C. Patel

*Massachusetts Institute of Technology, Department of Mechanical Engineering, Cambridge, MA 02139-4307, USA*

Received 4 August 1998; accepted 6 January 1999

**Abstract**

We present a new mechanistic model for the self-similar propagation of case II sorption fronts of diluents into glassy polymers. The model not only presents a clear differentiation between the chemical-potential-induced driving forces and the material misfit-induced pressures that develop in the Fickian precursor field that counteract the driving forces but also set up conditions for visco-plastic extrusion of the diluent-enriched polymer out of the surface or into a zone of rubbery gel behind the case-II process front. The quantitative predictions of the model are capable of giving accurate comparisons with experimental measurements, particularly with those of Kramer and co-workers on the penetration of iodoalkanes into polystyrene. 

*Keywords*: Case II sorption; Non-Fickian diffusion; Diluent penetration into glassy polymers

## Nomenclature

$B$: Scale factor of activation free energy for strain rate in the plastic flow model of Argon–Bessonov
$D$: Diffusion constant of diluent in the glassy polymer
$I$: A dissipation integral as defined by Eq. (59)
$J$: Diluent flux across a cross section
$M_w$: Molecular weight of diluent
$R$: Universal gas constant
$V$: Velocity of case II sorption front
$Y$: Tensile plastic resistance at a given temperature, modified by plasticization effect
$Y_0$: Tensile plastic resistance at a given temperature
$a$: Activity of diluent in the glassy polymer
$m$: Plasticization factor
$n$: Exponent of effective (equivalent) stress in phenomenological representation of plastic strain rate
$p$: Pressure component of local stress tensor (a negative mean normal stress)
$s$: Athermal tensile plastic resistance, modified by plasticization effect
$s_0$: Athermal plastic resistance in the Argon–Bessonov model of polymer plasticity
$x$: Depth coordinate from initial position of free surface ($=x_1$)
$\chi$: Flory–Huggins interaction parameter of diluent with glassy polymer
$\Lambda$: Effective thickness of case II plastic process front
$\Omega$: Effective molar volume of diluent molecule
$\Pi$: Osmotic pressure
$\Sigma$: Osmotic suction
$\Theta$: Material dilatation
$\epsilon_s$: Misfit parameter of diluent molecule in glassy polymer
$\epsilon_{ij}$: Elements of total strain tensor
$\epsilon^e_{ij}$: Elements of elastic component of strain tensor
$\epsilon^p_{ij}$: Elements of plastic component of strain tensor
$\dot{\epsilon}_0(T)$: Pre-exponential rate factor in phenomenological plastic strain rate expression
$\dot{\epsilon}_{AB}$: Pre-exponential factor in plastic strain rate expression in the Argon–Bessonov model of plastic flow of glassy polymer
$\dot{\epsilon}^p_e$: Effective (equivalent) plastic strain rate
$\varphi(\xi)$: Diluent concentration at depth $\xi$ below advancing case II front
$\varphi_c$: Critical diluent concentration at advancing case II front in Fickian precursor region
$\varphi_e$: Diluent concentration in swollen gel behind case II front (or in the environment in equilibrium)
$\varphi_o$: Background diluent concentration in glassy polymer
$\mu$: Shear modulus
$\mu_c$: Chemical potential of diluent in glassy polymer
$\nu$: Poisson's ratio
$\rho$: Density of diluent

* Corresponding author. Tel.: + 1-617-2532217; fax: + 1-617-2588742.
*E-mail address:* oona@mit.edu (A.S. Argon)

0032-3861/99/$ - see front matter 
PII: S0032-3861(99)00033-6

$\sigma_e$: von Mises tensile effective (equivalent) stress
$\sigma_m$: Mean normal stress component of stress tensor $(-p)$
$\sigma_{ij}$: Elements of stress tensor
$\xi$: Coordinate of material point away from advancing case II front, into Fickian region
$\eta$: $(=\sigma_e/s)$
$\zeta$: $(=V\xi/D)$
$(\cdot)$: Time derivative

## 1. Introduction

Glassy polymers have a large capacity to sorb diluents without dissolving, and transforming in the process from a stiff solid to a rubbery gel. Unlike the Fickian diffusion of an isotope of an elemental solid into the corresponding pure substance, which is accompanied by negligible material misfit, the penetration of a diluent molecule into a glassy polymer is accompanied by a very substantial material misfit. As a consequence, while the Fickian diffusional penetration of an isotope obeys a $t^{1/2}$ time law at constant temperature and progressively slows down, the diluent-laden gel penetrates into the glassy polymer as a sharp front and continues to advance linearly with time. This latter sorption process that has been termed case II diffusion by Alfrey et al. [1] has received much attention over the years. Both its phenomenology and its kinetics have been explored extensively, and theoretical models of varying sophistication have been developed. The theoretical model formulated by Thomas and Windle [2] (TW) has identified the principal mechanisms of the process as being driven by an activity or chemical potential difference between the glassy polymer and the diluent in contact with it, and that the rate of penetration of the diluent is governed by the deformation resistance of the solid polymer that was considered to be its viscosity-albeit modified by the plasticization effect of the sorbed diluent. Leading into their model, TW also provide a review of the definitive work of earlier investigators, up to the time of their own model. A more expanded discussion of these earlier developments was given by Windle [3]. The TW model has stimulated much definitive experimental research of case II sorption, particularly by Kramer and coworkers [4–6] on a number of polymer/diluent systems using the Rutherford backscattering technique. Of these, the systematic study involving the sorption of a series of iodoalkanes, ranging from iodopropane to iodooctane into PS has given the most definitive insight into the complex kinetics of the case II sorption process and provided the means for the most detailed evaluation of the TW model. These experiments have, moreover, stimulated further more detailed theoretical developments of the TW model. Thus, Hui et al. [7–9] have dealt with both the initial transient penetration of the diluent and the final steady state motion of the sorption front — all within the framework of the TW model. The experiments and these more detailed models showed that while the TW model furnishes a successful qualitative framework of most of the important mechanistic factors, it is unable to provide a quantitatively accurate statement of the kinetics of the diluent penetration, which requires a more highly non-linear material deformation resistance. Wu and Peppas [10] have sharpened the focus by noting that two kinetic processes jointly govern the case II process and their roles in the changing behavior of the process over a wide range of parameters should be characterizable by a diffusional Deborah number which gives the ratio of the mechanical relaxation time of the solid behavior to the diffusional relaxation time of the diluent in the glassy polymer. Thus, large Deborah numbers represent sorption processes controlled by mechanical relaxation and small ones (less than unity), controlled by the diffusional penetration rate of the diluent. Having stated this important scaling relation, however, Wu and Peppas proceeded with many of the same linearized response forms of the TW model.

More recently Rossi and coworkers [11,12] and Astarita and Sarti [13] considered the case II sorption process primarily in a formal sense of propagation of a sharp process front, separating material diffusional conductance differing by several orders of magnitude as would be expected for the swollen gel relative to that of the solid glassy polymer. There has been a number of other model developments of case II sorption such as, e.g. of Govindjee and Simo [14] that has emphasized the representation of the thermodynamic driving forces arising from activity gradients and a glass-to-rubber transition but still dealing with the material deformation resistances by viscoelastic formalisms. Other models have been adequately referred to in the aforementioned studies and will not be recalled here further.

As a distinguishing feature of case II sorption is the associated material misfit produced by the sorbed diluent, the development of internal stresses must be an important component of the process. Alternatively, there must be present possible effects of applied external stresses or pressures accelerating or retarding the diluent penetration. Thus, TW have noted that the presence of an imposed negative pressure will significantly enhance the equilibrium solubility of the diluent in the glassy polymer at a given temperature, which should accelerate the penetration. This aspect was used by Brown et al. [15] and subsequently by Argon et al. [16] to explain diluent induced toughening of certain glassy polymers through the effect of the diluent on crazing. A more direct application of the effect of an out-of-surface tensile stress was considered by Brown [17] in accelerating case II sorption as a possible mechanism of solvent crazing of glassy polymers. Finally, the effect of applied tensile or compressive bi-axial stresses in the surface layers, on influencing case II diffusion was experimentally explored by Nealey et al. [18] in the Ultem/RDP system by bi-axial bending of thin disks of the RDP-covered Ultem through Rutherford back scattering experiments. However, no measurable effects were found, much against best expectations, possibly because of the accompanying relaxation of the applied stresses in the bent disks.

The developments to be presented in the present communication were stimulated by the findings of the diluent induced toughening effects in glassy polystyrene, discovered by Gebizlioglu et al. [19] that have led to the diluent accelerated crazing model discussed by Argon et al. [16]. Here we consider primarily the conditions that govern the self-similar propagation of fully developed case II sorption fronts, associated with their Fickian precursors. The principal point of departure from all other models will be the specific considerations of the effects of the diluent induced substantial material misfit and the non-linear visco-plastic response of the constrained glassy polymer matrix to the misfit induced effective (von Mises) stresses, leading eventually to a plastic ejection of a relaxed gel through a narow bi-axial process zone of the advancing case II front. Our object is to demonstrate that the self similar advance of the case II front, with a constant velocity, is governed in a balanced measure by both the kinetics of the diffusional penetration of the diluent and the kinetics of visco-plastic flow of the diluent-plasticized glassy polymer. We demonstrate that the processes termed *anomolous diffusion* and *case II diffusion* are one and the same and are smoothly connected. A transition from the former to the latter occurs in a narrow range of increase of chemical potential of the diluent and the associated sharp increases in visco-plastic distortional strain rates in the glassy polymer undergoing its final stages of swelling.

In Section 2 we introduce our model of penetration of the diluent into a half space of glassy polymer in the form of planar fronts, in response to an imposed diluent activity difference between the surrounding environment and the bulk of the glassy polymer, and develop the special forms of the coupled diffusion and elasto-visco-plastic deformation rates associated with the self similar propagation front. We discuss first the details of case II sorption fronts only in response to the stresses induced by the material misfit produced by the penetrating diluent and then consider the very important accelerating effects of an out-of-surface tensile stress that is present e.g. in the border zones of crazes.

In Section 3 we calculate a number of steady state case II penetration scenarios, with a particular emphasis to match the detailed case II sorption measurements of Gall et al. [6] on the penetration of a series of iodoalkanes into polystyrene.

Finally, in Section 4 we compare our predictions with the measurements of Gall et al. and discuss other applications of the model, such as the limited supply diffusion experiments of Nealey et al. [18] with gradually decreasing diluent penetration velocities associated with decreasing levels of chemical potential.

## 2. Theoretical model

### 2.1. Problem statement

The tendency of a diluent to penetrate into, or being sorbed by, a glassy polymer is considered by the thermodynamics of osmosis through a semi-permeable membrane [20]. In the context of our development we view the surface of the glassy polymer (and later the thin process layer of the case II sorption front) as this semi-permeable membrane. The sorption is governed by the level of activity $a$ of the diluent, defined through the chemical potential $\mu_c$ as:

$$a = \exp\left(\frac{\mu_c}{RT}\right). \tag{1}$$

In the present case of a system of a diluent and a glassy polymer, activity of the diluent is described by the diluent concentration $\varphi_e$ in a more specific expression given as:

$$a = \varphi_e \exp(1 - \varphi_e) \exp\{\chi(1 - \varphi_e)^2\}, \tag{2}$$

where $\varphi_e$ represents the equilibrium concentration of the diluent in contact with the half space of the glassy polymer, $\chi$ is the Flory–Huggins interaction parameter (which is taken to be zero for good solvents). In very dilute systems the activity simplifies to:

$$a = \varphi_e \exp(1 - \varphi_e) \rightarrow k\varphi_e. \tag{3}$$

If the diluent at a concentration of $\varphi_e$ is placed in contact with a glassy polymer containing only a background concentration $\varphi_0$ of diluent, there will be a strong "driving force" on the diluent to cross the semi-permeable membrane (the surface) into the solid polymer.

We will find it convenient to represent this driving force on the diluent to cross the semi-permeable membrane, arising from the large difference of activity (concentration difference) of the diluent between that in the environment and that in the glassy polymer by a thermodynamic notion that we label as the *osmotic suction*, $\Sigma$, (a negative pressure) defined as:

$$\Sigma = \frac{RT}{\Omega} \ln \frac{\varphi_e}{\varphi_0}, \tag{4}$$

where $\Omega$ is the effective molar volume of the diluent (partial molar volume if the environment consists of several components). We note that $\Sigma$ is merely a thermodynamic "driving force" that we might view like a negative pressure. The solid experiencing $\Sigma$ is not stressed. In the thermodynamics of osmosis this tendency is defined in the opposite sense by stating that the large difference in concentration of the diluent between that in the environment and that in the glassy polymer *can be maintained in check* if the solid is placed under a real pressure $\Pi$ known as the *osmotic pressure*, (a negative mean normal stress) defined by:

$$\Pi = -\frac{RT}{\Omega} \ln \frac{\varphi_e}{\varphi_0}. \tag{5}$$

Thus, by definition, the application of such a pressure results in osmotic equilibrium, maintaining the large difference of diluent concentration indefinitely without any diluent

crossing the semi-permeable membrane.[1] We state this equilibrium as:

$$\Sigma + \Pi = 0. \tag{6}$$

We note that both $\Sigma$ and $\Pi$ are scalars and have the dimensions of "stress" or pressure. Thus, the osmotic pressure, as properly defined earlier, is not a "driving force" as has been stated by most investigators following TW, but rather a "retarding force", counteracting sorption. When an osmotic pressure is absent there is present a thermodynamic driving force arising from the concentration difference (i.e. an osmotic suction), which promotes penetration of diluent across the semi-permeable membrane. The sorption of the diluent by the glassy polymer occurs through the establishment of a Fickian diffusion front in which the rate of penetration of the diluent is governed by the diffusion constant $D$ of the diluent in the glassy polymer. Such penetration, first as a transient front, has been analysed by several investigators [7–9]. We will not pursue this transient diluent behavior, but rather concentrate our attention only on the sharp fronts (the case II sorption front) propagating self-similarly with a given diluent concentration profile at a constant velocity $V$.

The diffusional penetration of the diluent into the glassy polymer creates material misfit, which can be estimated in an idealized sense through the solution of the problem of a spherically misfitting volume element in a finite elastic solid. When such dilatational misfit is introduced into the half space of the glassy polymer, planar material layers parallel to the surface can not expand freely in their plane because of the constraint imposed by the semi-infinite substrate. This sets up bi-axial compression in the planar layers, permitting however, the layers to elastically expand perpendicular to the surface. The resulting bi-axial stress state has a deviatoric (von Mises) component, as well as a pressure component, both of which increase monotonically in the direction of increasing diluent concentration in the Fickian precursor front. The pressure component $p$ of the misfit strain field will begin to counteract the *osmotic suction*, while the deviatoric component will bring the material progressively towards generalized plastic yield. If the initial diluent concentration difference is such that bi-axial visco-plastic response is initiated while $\Sigma - p > 0$ a case II sorption front can form, extruding plastically, the diluent-enriched polymer backward, normal to the free surface.[2] This represents a necessary condition for the initiation of a case II sorption front from a free surface, but may be insufficient for the development of a self-similarly propagating front, leaving behind a swollen gel. For this second requirement to be satisfied the diluent concentration in the plastically extruded material must also be sufficient to lower the glass transition temperature of the ejected diluent-laden material to be below the ambient temperature to transform into a gel with negligible deformation resistance, as was demonstrated by Nealey et al. [18] (see Section 4.3). When this second requirement cannot be met, the case II front can initiate at the free surface but cannot continue to propagate inward because the plastic resistance of the ejected material cannot be overcome, resulting in the build-up of an opposing stress that stalls the process front. In this case the successful inward propagation of the front requires raising the external diluent concentration $\varphi_e$ above the level of what would be required to accomplish the solid-to-gel transformation. Lasky et al. [4] furnish an excellent demonstration of this phenomenon in the polystyrene iodohexane system, showing that even though front motion can initiate from the free surface at a given surface concentration $\varphi_s$, inward propagation requires a higher $\varphi_e$ in what is to become the swollen gel behind the case II front.

Thus, we recognize that the condition for plastic extrusion must coincide with a transformation of the extrudate into a rubbery gel when it is released from the constraint of the substrate. If the condition of $\Sigma - p = 0$ is reached before the deviatoric (von Mises) stress in the Fickian precursor field at the surface layers reaches general yield, a case II front will not develop at all as the misfit induced pressure will have fully compensated the driving force due to the chemical potential difference and has become equal to the osmotic pressure. The latter condition occurs when the surface diluent concentration is too low.

Several other conditions need also to be noted before a comprehensive model for the self-similar propagation of the swelling front can be stated. First, as the sorbed diluent concentration $\varphi$ ($\xi$) increases in the Fickian precursor field in the glassy polymer, where $\xi$ represents the coordinate of the point away from the surface (or the advancing case II front) the local plastic resistance of the polymer will significantly decrease due to a diluent-induced plasticization effect where the penetrated diluent molecules monotonically reduce the interaction between molecular segments of the glassy polymer.

Finally, for applications of the case II sorption process to the solvent crazing response of a glassy polymer, the tension in the craze tufts will impose an out-of-surface tensile stress to the local case II process front at the craze border. This will significantly enhance the deviatoric (von Mises) component of the stress in the precursor field and will help promote an early transition from elastic to plastic behavior as noted first by Brown [17].

As mentioned earlier, we will develop our model for the case II front only for the condition of self-similar propagation with a constant built-in diluent concentration profile. While these developments are fully capable of dealing also with any transient response, the available material information is too inadequate to make such developments have much meaning.

[1] In this communication we use the terminology of *osmotic pressure* only in this defined sense, as the local pressure that stops transfer of diluent across the semi-permeable membrane—the external surface.

[2] Here, and in the following case II model, the term $p$ refers to the pressure component of a local stress tensor, which, by definition is a negative mean normal stress $\sigma_m$. Thus $p = \sigma_m = (\sigma_{11} + \sigma_{22} + \sigma_{33})/3$.

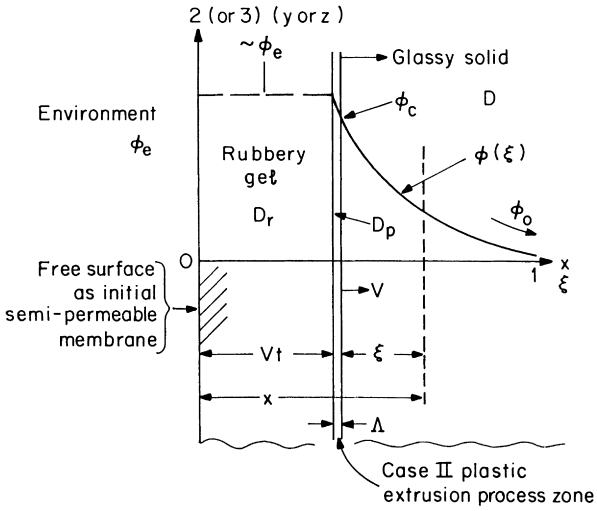


Fig. 1. Operational model parameters of a self-similarly advancing case II sorption process front.

### 2.2. Case II sorption front driven only by material misfit

Fig. 1 defines the parameters of a self-similarly advancing case II sorption front into a semi infinite glassy polymer substrate containing an initial diluent concentration $\varphi_0$ at a trace level. A Fickian precursor diffusion front with a characteristic concentration profile $\varphi(\xi)$ precedes the case II sorption front where $\xi$ is the coordinate of any point in the case II front field advancing with a constant velocity $V$ into the semi-infinite substrate. The case II process front is of thickness $\Lambda$ across which a concentration jump occurs from $\varphi_c$, the critical diluent concentration on the diluent-enriched glassy polymer substrate side to $\varphi_e$, the diluent concentration just behind the case II front in the swollen gel side. The concentration gradient of diluent in the swollen gel is considered to be negligible in comparison to the gradients in the Fickian precursor field, implying that the diffusion constant of the diluent in the gel is orders of magnitude larger than that in the diluent-enriched Fickian precursor zone. The diluent flux across the case II process layer is continuous with that just at the back end of the Fickian precursor zone.

If the diffusion constant $D$ in the Fickian field is independent of concentration, as experimental measurements of the front shape suggest, the concentration of diluent in the Fickian front will be [21].

$$\varphi(\xi) = \varphi_c \exp(-V\xi/D), \tag{7}$$

where $\varphi_c$ is the critical diluent concentration at the back end of the Fickian precursor field.

The material response in the Fickian field is described by two coupled rate equations in the two principal directions, 2 (and 3), in planes parallel to the case II front and, 1, perpendicular to the front.

As no out-of-surface stress $\sigma_{11}$ is applied to the front in most cases and as no shear stresses exist in the principal coordinate field, 1 and 2, the differential equation of equilibrium becomes:

$$\frac{\partial \sigma_{11}}{\partial x_1} = 0 \tag{8}$$

giving $\sigma_{11} = 0$ for all depth coordinates.

As the substrate is of semi-infinite extent, the total strains and strain rates in the 2 and 3 directions must vanish, i.e.

$$\epsilon_{22} = \epsilon_{33} = 0, \tag{9a}$$

$$\dot{\epsilon}_{22} = \dot{\epsilon}_{33} = 0, \tag{9b}$$

giving a basic rate equation in the 2 direction (also 3 direction) of

$$\dot{\epsilon}_{22} = 0 = \dot{\epsilon}^{e}_{22} + \dot{\epsilon}^{p}_{22} + \frac{\dot{\Theta}}{3}, \tag{10}$$

where $\dot{\epsilon}^{e}_{22}$ is the elastic strain rate, $\dot{\epsilon}^{p}_{22}$ the plastic strain rate and $\dot{\Theta}$ the dilatation rate due to the rate of insertion of material misfit, and, of course, dots above symbols mean time derivatives.

By generalized Hooke's law of elastic response

$$\dot{\epsilon}^{e}_{22} = \left(\frac{1-\nu}{1+\nu}\right)\frac{\dot{\sigma}_{22}}{2\mu}, \tag{11}$$

where $\mu$ is the shear modulus and $\nu$ the Poisson's ratio of the glassy polymer, which we consider to be constant.

We consider the deviatoric plastic response of the glassy polymer to be given by a convenient power-law representation of

$$\dot{\epsilon}^{p}_{e} = \dot{\epsilon}_0(T)(\sigma_e/s)^n, \tag{12}$$

where $\dot{\epsilon}^{p}_{e}$ and $\sigma_e$ stand for the von Mises deviatoric (effective) plastic strain rate and von Mises effective stress respectively. The more mechanistically sound form of the inelastic response is given by a proper Arrhenius rate expression discussed in detail by Argon [22] with a stress dependent activation energy, for which the expression in Eq. (12) represents a functional fit to this form as discussed in Appendix A. In Eq. (12) $s$ stands for the tensile (athermal) reference plastic resistance of the glassy polymer that will be taken to be dependent on diluent concentration, $\dot{\epsilon}_0(T)$ is a strain rate pre-factor and $n$ is a phenomenological exponent. Both $\dot{\epsilon}_0(T)$, and $n$ are temperature dependent in a well defined way, as developed in Appendix A where the aforementioned form is related to the mechanistically preferable Arrhenius form of the Argon–Bessonov model of plastic flow of a glassy polymer.

The material dilatation $\Theta$, associated with the sorbed diluent producing swelling, is given by elasticity for a misfitting sphere (for a finite solid with free surfaces) [23] as,

$$\Theta = 9\epsilon_s\varphi, \tag{13a}$$

and in rate form as

$$\dot{\Theta} = 9\epsilon_s\dot{\varphi}, \tag{13b}$$

where $e_s = \Delta r/r_0$ is the linear misfit parameter, considering the sorbed diluent molecule idealized as a sphere of radius $r_0 + \Delta r$ inserted into a spherical cavity of radius $r_0$ of the glassy polymer. Clearly, this is a convenient abstraction, as the actual diluent molecule in the glassy polymer will have, most likely, a complex non-spherical shape. Misfit parameters in equilibrium-sorbed polymer systems are readily measurable [24]. For systems of interest to us, however, they have not been measured and will be estimated from the transient response of the Fickian front in a manner discussed in Section 3.1.

By virtue of time invariance of the structure of the self-similarly advancing Fickian front

$$\dot{\sigma}_{22} = -V\frac{\partial \sigma_{22}}{\partial \xi} \tag{14}$$

giving

$$\dot{\epsilon}^{e}_{22} = -\left(\frac{1-\nu}{1+\nu}\right)\frac{V}{2\mu}\frac{\partial \sigma_{22}}{\partial \xi}. \tag{15}$$

From the associated flow rule the inelastic strain rate component is [23],

$$\dot{\epsilon}^{p}_{22} = \frac{1}{2}\frac{\dot{\epsilon}^{p}_{e}}{\sigma_e}\sigma_{22}, \tag{16}$$

moreover

$$\frac{\dot{\Theta}}{3} = 3\epsilon_s\dot{\varphi} = -3\epsilon_s V\frac{\partial \varphi}{\partial \xi} \tag{17a}$$

giving

$$\frac{\dot{\Theta}}{3} = \frac{3\epsilon_s\varphi_c V^2}{D}\exp\left(-\frac{V\xi}{D}\right). \tag{17b}$$

Similarly, in the 1 direction, in which the swelling material can expand, we have for the total strain rate

$$\dot{\epsilon}_{11} = \dot{\epsilon}^{e}_{11} + \dot{\epsilon}^{p}_{11} + \frac{\dot{\Theta}}{3}, \tag{18}$$

with individual terms taking the forms of:

$$\dot{\epsilon}^{e}_{11} = -\frac{\nu}{(1+\nu)}\frac{\dot{\sigma}_{22}}{\mu} = \frac{\nu}{(1+\nu)}\frac{V}{\mu}\frac{\partial \sigma_{22}}{\partial \xi}, \tag{19a}$$

$$\dot{\epsilon}^{p}_{11} = -\frac{\dot{\epsilon}^{p}_{e}}{\sigma_e}\sigma_{22}, \tag{19b}$$

$$\frac{\dot{\Theta}}{3} = \frac{3\epsilon_s\varphi_c V^2}{D}\exp\left(-\frac{V\xi}{D}\right), \tag{19c}$$

with the particularly simple local stress states

$$\sigma_{11}(\xi) = 0 \qquad \text{and} \qquad \sigma_{22}(\xi) = \sigma_{33}(\xi),$$

the deviatoric (effective) stress $\sigma_e$ becomes

$$\sigma_e \equiv \{\tfrac{1}{2}[(\sigma_{22}-\sigma_{33})^2 + (\sigma_{33}-\sigma_{11})^2 + (\sigma_{11}-\sigma_{22})^2]\}^{1/2} = |\sigma_{22}(\xi)|. \tag{20}$$

Collecting the various terms together, gives the two rate expressions in the 2 direction and the 1 direction, respectively, as:

$$\dot{\epsilon}_{22} = \frac{(1-\nu)}{2(1+\nu)}\frac{V}{\mu}\frac{\partial \sigma_{22}}{\partial \xi} + \frac{\dot{\epsilon}^{p}_{e}}{2\sigma_e}\sigma_{22} + 3\epsilon_s\varphi_c\frac{V^2}{D} \times \exp\left(-\frac{V\xi}{D}\right) = 0 \tag{21}$$

(in the 2 direction), and

$$\dot{\epsilon}_{11} = \frac{\nu}{(1+\nu)}\frac{V}{\mu}\frac{\partial \sigma_{22}}{\partial \xi} - \frac{\dot{\epsilon}^{p}_{e}}{\sigma_e}\sigma_{22} + 3\epsilon_s\varphi_c\frac{V^2}{D}\exp\left(-\frac{V\xi}{D}\right) \tag{22}$$

(in the 1 direction), where $\dot{\epsilon}^{p}_{e}(\sigma_e)$ is a highly non-linear function of the effective stress as indicated in Eq. (12). Noting that $\sigma_e$ can be taken either + or −, and $\sigma_{22} < 0$, we have

$$\dot{\epsilon}_{22} = \frac{(1-\nu)}{2(1+\nu)}\frac{V}{\mu}\frac{\partial \sigma_e}{\partial \xi} - \frac{1}{2}\dot{\epsilon}^{p}_{e}(\sigma_e) + 3\epsilon_s\varphi_c\frac{V^2}{D} \times \exp\left(-\frac{V\xi}{D}\right) = 0, \tag{21a}$$

$$\dot{\epsilon}_{11} = -\frac{\nu}{(1+\nu)}\frac{V}{\mu}\frac{\partial \sigma_e}{\partial \xi} + \dot{\epsilon}^{p}_{e}(\sigma_e) + 3\epsilon_s\varphi_c\frac{V^2}{D}\exp\left(-\frac{V\xi}{D}\right), \tag{22a}$$

where $\partial\sigma_e/\partial\xi < 0$ in the Fickian misfit field.

### 2.3. Case II sorption front driven by material misfit and an out-of-surface tensile stress

As noted first by Brown [17], the presence of an out-of-surface tensile stress, in conjunction with a misfit-driven case II sorption front, finds important application in the solvent crazing phenomenon. The treatment of Brown, however, incorporates the same shortcoming of the TW model, which did not distinguish between a chemical potential (osmotic suction), induced "driving force" and a genuine pressure resulting from the misfiting sorbed diluent. In this section we generalize on the model presented in the previous section to account for the out-of-surface tensile stress.

We note that by virtue of equilibrium, as stated in Eq. (8) the application of an out-of-surface tensile stress in the principal coordinate system of 1–3, without shear stresses present, will be transmitted into the semi-infinite solid without change, i.e. $\sigma_{11}$ in the interior will be independent of $x$ (or $\xi$). Then, the expressions corresponding to those in Section 2.2 will change into

$$\epsilon^{e}_{11} = \frac{1}{(1+\nu)}\frac{\sigma_{11}}{2\mu} - \frac{2\nu}{(1+\nu)}\frac{\sigma_{22}}{2\mu}, \tag{23a}$$

$$\epsilon^{e}_{22} = \frac{(1-\nu)}{(1+\nu)}\frac{\sigma_{22}}{2\mu} - \frac{\nu}{(1+\nu)}\frac{\sigma_{11}}{2\mu}, \tag{24a}$$

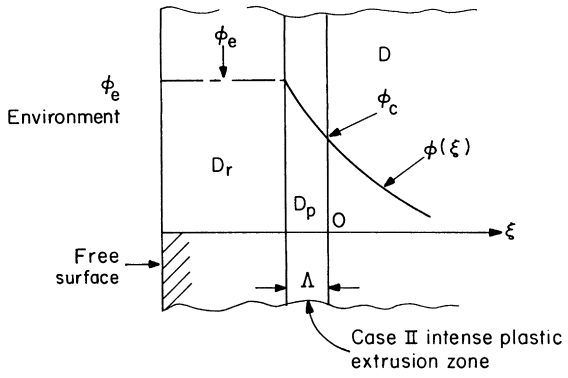


Fig. 2. Diluent flux border condition across the case II process front.

and the elastic strain rates into,

$$\dot{\epsilon}^{e}_{11} = -\frac{\nu}{(1+\nu)}\frac{\dot{\sigma}_{22}}{\mu}, \tag{23b}$$

$$\dot{\epsilon}^{e}_{22} = \left(\frac{1-\nu}{1+\nu}\right)\frac{\dot{\sigma}_{22}}{\mu} \tag{24b}$$

by virtue of the fact that $\dot{\sigma}_{11} = 0$.

The von Mises equivalent stress now becomes

$$\sigma_e = \pm(\sigma_{11} - \sigma_{22}), \tag{25}$$

giving rise to the corresponding plastic strain rate components:

$$\dot{\epsilon}^{p}_{11} = \frac{\dot{\epsilon}^{p}_{e}}{\sigma_e}(\sigma_{11} - \sigma_{22}) = \dot{\epsilon}^{p}_{e}, \tag{26}$$

$$\dot{\epsilon}^{p}_{22} = \frac{\dot{\epsilon}^{p}_{e}}{\sigma_e}\frac{1}{2}(\sigma_{22} - \sigma_{11}) = \frac{1}{2}\dot{\epsilon}^{p}_{e}. \tag{27}$$

The dilatation rate given by Eqs. (13b), (17a) and (17b) remains unaltered, as will be the self-similarity statement of the stress rate of Eq. (14).

In combining terms, we note that in the Fickian field $\sigma_{22} < 0$ and $\partial\sigma_{22}/\partial\xi > 0$. The final forms of the resulting equations for total strain rate in the 2 and 1 directions become

$$\dot{\epsilon}_{22} = -\left(\frac{1-\nu}{1+\nu}\right)\frac{V}{\mu}\frac{\partial\sigma_{22}}{\partial\xi} - \dot{\epsilon}^{p}_{e} + 6\epsilon_s\varphi_c\frac{V^2}{D} \times \exp\left(-\frac{V\xi}{D}\right) = 0, \tag{28}$$

$$\dot{\epsilon}_{11} = \frac{\nu}{1+\nu}\frac{V}{\mu}\frac{\partial\sigma_{22}}{\partial\xi} + \dot{\epsilon}^{p}_{e} + 3\epsilon_s\varphi_c\frac{V^2}{D}\exp\left(-\frac{V\xi}{D}\right). \tag{29}$$

We again note that

$$\frac{\partial\sigma_e}{\partial\xi} = -\frac{\partial\sigma_{22}}{\partial\xi} \text{ as } \frac{\partial\sigma_e}{\partial\xi} < 0,$$

while $\sigma_{22} < 0$ and $\dfrac{\partial\sigma_{22}}{\partial\xi} > 0$,

and that $\partial\sigma_{11}/\partial\xi = 0$ as recognized earlier, as $\sigma_{11}$ is externally applied and is not of material misfit origin. Then, the two principal total strain-rate expressions become

$$\dot{\epsilon}_{22} = \frac{(1-\nu)}{(1+\nu)}\frac{V}{\mu}\frac{\partial\sigma_e}{\partial\xi} - \dot{\epsilon}^{p}_{e}(\sigma_e) + 6\epsilon_s\varphi_c\frac{V^2}{D} \times \exp\left(-\frac{V\xi}{D}\right) = 0, \tag{28a}$$

$$\dot{\epsilon}_{11} = -\frac{\nu}{(1+\nu)}\frac{V}{\mu}\frac{\partial\sigma_e}{\partial\xi} + \dot{\epsilon}^{p}_{e}(\sigma_e) + 3\epsilon_s\varphi_c\frac{V^2}{D}\exp\left(-\frac{V\xi}{D}\right). \tag{29a}$$

We note that these two expressions are identical to (21a) and (22a) of the purely material misfit driven sorption process, where however, the effective stress $\sigma_e$ incorporates the out-of-surface tensile stress $\sigma_{11}$, which enters specifically only in the inelastic strain rate constitutive relation given by the second term in these equations. The gradient of the effective stress appearing in the first term is the same as it comes only from the misfit field. The tensile stress $\sigma_{11}$ has no gradient.

### 2.4. Plasticization of the glassy polymer by the diluent

The athermal reference tensile plastic resistance $s_0$ of the glassy polymer will be significantly lowered by the sorbed diluent as it reduces the intermolecular interactions. Often this reduction is taken to be of exponential form as [2]

$$s = s_0\exp(-m\varphi), \tag{30}$$

where we take $s_0$ as the athermal reference plastic resistance of the initial unmodified polymer. We will consider $m$ as adjustable and determine its magnitude by "tuning-in" the model to certain features of the experimental information. Here we recall that the athermal plastic resistance, dependent only on the slightly temperature dependent shear modulus, forms the basis of the kinetical statement of thermally activated plastic relaxations as discussed by Argon [22,25].

### 2.5. Diluent flux border condition

The critical diluent concentration $\varphi_c$ at the case II process front where plastic extrusion of the swollen and compressed diluent-enriched glassy polymer occurs in the reverse direction, diluent flux continuity must be present. Thus, $\varphi_c$, while scaling the processes in the Fickian precursor, is not an independent material property but depends on the driving forces produced by the chemical potential difference imposed by the surrounding environment. This connection to the external diluent concentration $\varphi_e$ in the surroundings is established by the condition of diluent flux continuity. As Fig. 2 depicts, in the zone just behind the case II process front of thickness $\Lambda$ the diffusion constant of the diluent, $D_r$ is orders of magnitude larger than the diffusion consistent $D$ of the Fickian precursor field. Therefore, for the purpose of our application we take the diluent concentrations on the

back border of the case II process front to be $\varphi_e$, the equilibrium concentration of the diluent in the environment (or what it is as applied to the surface). Clearly, the diffusion constant $D_p$ in the case II front of thickness $\Lambda$ itself must be intermediate in magnitude between $D$ and $D_r$, as we take the constitution of material in the case II process front to be similar to that of the glassy polymer ahead of the front we arbitrarily consider $D_p$ to be $D$. Then, the diluent flux continuity across the case II process front requires that

$$J = \frac{D(\varphi_e - \varphi_c)}{\Lambda\Omega} = -\frac{D}{\Omega}\left(\frac{\partial\varphi}{\partial\xi}\right)_{\xi=0} \tag{31}$$

where $\Omega$ is again the molar volume of the diluent as, however,

$$\left(\frac{\partial\varphi}{\partial\xi}\right)_{\xi=0} = -\varphi_c\frac{V}{D} \tag{32}$$

we obtain

$$\varphi_c = \varphi_e\frac{1}{\left(1 + \dfrac{\Lambda V}{D}\right)}. \tag{33}$$

As the levels of $\varphi_e$ and $\varphi_c$ have been reported in the experiments of Kramer and coworkers [4,5] together with the case II front velocities it is possible to estimate the case II process front thickness $\Lambda$ for the systems dealt with by them.

For example in the system of iodohexane, being sorbed into PS, Gall et al. [6] report that for a diluent activity level $a = 0.45$ ($\varphi_e = 0.203$)[3] in the environment, the critical concentration $\varphi_c = 0.14$ at the case II sorption front where the front velocity is $V = 10^{-2}$ nm/s and the diffusion constant is $10^{-13}$ cm$^2$/s (all at room temperature). From here we estimate that $\Lambda = 0.45$ μm which we consider to be quite acceptable-albeit intuitively to some extent on the high side.

### 2.6. Case II front velocity in a model with abrupt elastic-to-plastic transition

The two, coupled total strain rate expressions without an out-of-surface stress $\sigma_{11}$ (Eqs. (21a) and (22a)) and with an out-of-surface stress (Eqs. (28a) and (29a)) are highly nonlinear if the inelastic strain rate expression of Eq. (12) is considered everywhere in the Fickian precursor field. A much simpler and quite insightful solution of these equations to determine expressions for the case II front velocity can be obtained by considering a simplified response first, in which the elastic-to-plastic (e–p) transition occurs abruptly and only inside the case II process zone of thickness $\Lambda$. In this model until $\sigma_e$ reaches a critical value the inelastic strain rates are considered to be zero and the two total strain rate expressions simplify considerably.

We consider first the case where $\sigma_{11} = 0$. Then

$$\dot{\epsilon}_{22} = \left(\frac{1-\nu}{1+\nu}\right)\frac{V}{\mu}\frac{\partial\sigma_e}{\partial\xi} + 6\epsilon_s\varphi_c\frac{V^2}{D}\exp\left(-\frac{V\xi}{D}\right) = 0 \tag{34}$$

$$\dot{\epsilon}_{11} = \frac{\partial v_\xi}{\partial\xi} = \frac{\nu}{1+\nu}\frac{V}{\mu}\frac{\partial\sigma_e}{\partial\xi} + 3\epsilon_s\varphi_c\frac{V^2}{D}\exp\left(-\frac{V\xi}{D}\right), \tag{35}$$

with

$$\dot{\varphi} = \varphi_c\frac{V^2}{D}\exp\left(-\frac{V\xi}{D}\right) \tag{36}$$

remaining intact, where $v_\xi$ is the material-point velocity in the moving field of the Fickian front. We note first that at $\xi = 0$ at the entry into the case II process zone

$$\dot{\varphi}(0) = \varphi_c\frac{V^2}{D}. \tag{37}$$

This simple expression, which is the consequence of the self-similarity statement of the advancing case II front has been considered by Kramer and coworkers [6–9] as being a result of the TW sorption model in which the distinction is blurred between an *osmotic suction* (chemical potential or activity difference) as a "driving force" and a *pressure* (consequence of diluent induced material misfit) that tends to counteract it. Thus, the impressive agreement of the experimental measurements of Gall et al. [6] with the form of Eq. (37) is a consequence of only self-similarity and makes no statement on the accuracy of the TW model.

Both Eqs. (34) and (35) can be integrated in the Fickian front between $\xi = 0$ and $\xi = \infty$, giving

$$\left(\frac{1-\nu}{1+\nu}\right)\frac{V}{\mu}\sigma_e(\xi) - 6\epsilon_s\varphi_c V\exp\left(-\frac{V\xi}{D}\right) + C_1 = 0, \tag{38}$$

and

$$v_\xi(\xi) = -\frac{\nu}{(1+\nu)}\frac{V}{\mu}\sigma_e(\xi) - 3\epsilon_s\varphi_c V\exp\left(-\frac{V\xi}{D}\right) + C_2. \tag{39}$$

As $\sigma_e(\xi)$ and $v_\xi(\xi)$ both vanish at $\xi = \infty$ we have,

$$C_1 = C_2 = 0$$

giving

$$\left(\frac{1-\nu}{1+\nu}\right)\frac{\sigma_e(0)}{\mu} - 6\epsilon_s\varphi_c = 0, \tag{40}$$

$$\frac{v_\xi(0)}{V} = -\frac{\nu}{(1+\nu)}\frac{\sigma_e(0)}{\mu} - 3\epsilon_s\varphi_c, \tag{41}$$

where now $v_\xi(0)$ is the velocity of the material points going through the case II front. From Eqs. (40) and (41) we have,

$$\sigma_e(0) = 6\epsilon_s\varphi_c\mu\left(\frac{1+\nu}{1-\nu}\right), \tag{42}$$

[3] The case II front begins to advance at concentrations $\varphi_e$ in the gel, less than $\varphi_e = 0.203$ in the external environment, but fully developed case II fronts require elevation of $\varphi_e$ asymptotically up to the equilibrium value given earlier. See also Section 4.1.

and also

$$\frac{v_{\xi}(0)}{V} = -3\epsilon_s\varphi_c\left(\frac{1+\nu}{1-\nu}\right). \tag{43}$$

Moreover, from Eqs. (34) and (35) we also have for the total strain rate in the sorption direction

$$\dot{\epsilon}_{11} = 3\epsilon_s\dot{\varphi}\left(\frac{1+\nu}{1-\nu}\right). \tag{44}$$

Now, we note that at a certain critical level of the effective stress $\sigma_e$ when plastic response is abruptly initiated the aforementioned total plastic strain rate at the case II process front must become entirely a plastic strain rate by the assumed condition of an abrupt elastic to plastic transition. Then "material-points" will go through the case II process front and will be ejected backward (as a swollen gel). Thus from Eq. (44) we have at $\xi = 0$

$$\dot{\varphi}(0) = \frac{1}{3\epsilon_s}\left(\frac{1-\nu}{1+\nu}\right)\dot{\epsilon}_{11}, \tag{45}$$

and

$$\dot{\epsilon}_{11} \rightarrow \dot{\epsilon}^{p}_{11} = \dot{\epsilon}_e = \dot{\epsilon}_0(T)\left(\frac{\sigma_e(0)}{s}\right)^n = \dot{\epsilon}_0(T)\left(\frac{6\epsilon_s\varphi_c\mu}{s(\varphi_c)}\left(\frac{1+\nu}{1-\nu}\right)\right)^n, \tag{46}$$

which results from $\sigma_{22} = \sigma_e$, giving for the critical rate of increase of diluent concentration at $\xi = 0$.

$$\dot{\varphi}(0) = \frac{\dot{\epsilon}_0(T)}{3\epsilon_s}\left(\frac{1-\nu}{1+\nu}\right)\left(\frac{6\epsilon_s\varphi_c\mu}{s(\varphi_c)}\left(\frac{1+\nu}{1-\nu}\right)\right)^n. \tag{47}$$

Finally, through the use of Eq. (37) we have the case II front velocity:

$$V = \sqrt{\frac{2\dot{\epsilon}_0(T)D(T)\mu}{s(\varphi_c)}\left(\frac{6\epsilon_s\varphi_c\mu}{s(\varphi_c)}\left(\frac{1+\nu}{1-\nu}\right)\right)^{n-1}}. \tag{48}$$

### *2.7. Thickening rate of the swollen gel material behind the case II front*

When the previously elastically compressed diluent-enriched material arrives at the case II front and is plastically extruded backward with a relative velocity $v_{\xi}(0)$, it is also considered to undergo an expansion transformation from solid to gel in which the material misfit becomes relaxed. This produces an expansion equal to the volume fraction of diluent arriving at the case II front, i.e. by $\varphi_c$, accompanied, incidentally with significant molecular alignment in the gel.

Thus, the thickening rate $\dot{L}_s$ of the swollen material gel should be

$$\dot{L}_s = (1+\varphi_c)v_{\xi}(0) = 3\epsilon_s\varphi_c(1+\varphi_c)\left(\frac{1+\nu}{1-\nu}\right)V. \tag{49}$$

### *2.8. Case II front velocity in a model with gradual elastic-to-plastic transition*

The model for the case II front presented in Section 2.6 neglects inelastic relaxation in the Fickian misfit field and considers the e–p transition only at the case II process front. While this led to a simple expression for well developed and rapidly moving case II fronts driven by substantial osmotic suction, it does not model well the cases of low velocity motion under smaller levels of osmotic suction that constitute the phenomenon of anomolous diffusion where the velocities are small but their increments with changes in chemical potential are large.

Dealing with such phenomena requires taking account of the inelastic relaxations in the Fickian region with a smooth and gradually accelerating inelastic strain rate as Eq. (12) indicates.

Thus, we return to the more general and complete expressions for the coupled total principal strain rates of Eqs. (21a) and (22a) for the case II fronts, driven entirely by the diluent induced material misfit. To facilitate the solution of the problem to obtain expressions for case II front velocity we introduce the dimensionless variables

$$\zeta = \frac{V\xi}{D}, \tag{51a}$$

and

$$\frac{\sigma_e}{s_0} = \eta, \tag{50b}$$

where $s_0$ is the unmodified athermal plastic resistance of the pure glassy polymer. With these dimensionless variables the two expressions for total principal strain rate become

$$\frac{\dot{\epsilon}_{22}}{\dot{\epsilon}_0} = \frac{1}{2}\left(\frac{1-\nu}{1+\nu}\right)\left(\frac{s_0}{\mu}\right)\left(\frac{V^2}{D\dot{\epsilon}_0}\right)\left(\frac{\partial\eta}{\partial\xi}\right) - \frac{1}{2}\frac{\dot{\epsilon}^{p}_0}{\dot{\epsilon}_0} + 3\epsilon_s\varphi_c\left(\frac{V^2}{D\dot{\epsilon}_0}\right)\exp(-\zeta) = 0, \tag{51}$$

$$\frac{\dot{\epsilon}_{11}}{\dot{\epsilon}_0} = \left(\frac{V^2}{D\dot{\epsilon}_0}\right)\left(\frac{\partial v_{\zeta}}{\partial\zeta}\right) = -\frac{\nu}{1+\nu}\left(\frac{s_0}{\mu}\right)\left(\frac{V^2}{D\dot{\epsilon}_0}\right)\left(\frac{\partial\eta}{\partial\zeta}\right) + \frac{\dot{\epsilon}^{p}_e}{\dot{\epsilon}_0} + 3\epsilon_s\varphi_c\left(\frac{V^2}{D\dot{\epsilon}_0}\right)\exp(-\zeta), \tag{52}$$

where $v_{\varphi}$ is a local material-point velocity in the moving coordinate system normalized with the case II front velocity.

Proceeding similarly to the developments of Section 2.6, integration of these two equations over the Fickian

precursor range from $\zeta = 0$ to $\zeta = \infty$ gives

$$-\left(\frac{1-\nu}{1+\nu}\right)\left(\frac{s_0}{\mu}\right)\left(\frac{V^2}{D\dot{\epsilon}_0}\right)\eta(0) - \int_0^\infty \left(\frac{\eta}{g(\varphi)}\right)^n \mathrm{d}\zeta + 3\epsilon_s\varphi_c\left(\frac{V^2}{D\dot{\epsilon}_0}\right) = 0 \tag{53}$$

$$-\left(\frac{V^2}{D\dot{\epsilon}_0}\right)v_\zeta = \left(\frac{\nu}{1+\nu}\right)\left(\frac{s_0}{\mu}\right)\left(\frac{V^2}{D\dot{\epsilon}_0}\right)\eta(0) + \int_0^\infty \left(\frac{\eta}{g(\varphi)}\right)^n \mathrm{d}\zeta + 3\epsilon_s\varphi_c\left(\frac{V^2}{D\dot{\epsilon}_0}\right). \tag{54}$$

In Eqs. (53) and (54) the non-linear visco-plastic rate relation of Eq. (12) was introduced and appears in the definite integrals.

The function $g(\varphi)$ is the attenuation factor of the effect of the diluent on the plastic resistance, i.e. $g(\varphi) = \exp(-m\varphi)$, presented in Section 2.4.

Evaluation of the total strain rate expressions of Eqs. (51) and (52) at $\zeta = 0$ and elimination of $(\partial\eta/\partial\xi)_{\zeta=0}$ from them, gives in terms of $\dot{\varphi}(0)$

$$\dot{\epsilon}_{11} = \left(\frac{1-2\nu}{1-\nu}\right)\dot{\epsilon}^{\mathrm{p}}_{\mathrm{e}}(0) + \left(\frac{1+\nu}{1-\nu}\right)3\epsilon_s\dot{\varphi}(0). \tag{55}$$

Moreover, recognizing again that in the case II process zone at $\zeta = 0$

$$\dot{\epsilon}_{11} = \dot{\epsilon}^{\mathrm{e}}_{11} + \dot{\epsilon}^{\mathrm{p}}_{11} \rightarrow \dot{\epsilon}^{\mathrm{p}}_{11} = \dot{\epsilon}^{\mathrm{p}}_0(0), \tag{56}$$

by virtue of the fact that $|\sigma_{\mathrm{e}}| = -\sigma_{22}$, we have,

$$\dot{\varphi}(0) = \frac{\nu}{(1+\nu)}\frac{\dot{\epsilon}^{\mathrm{p}}_{\mathrm{e}}}{3\epsilon_s} = \frac{\nu}{(1+\nu)}\frac{\dot{\epsilon}_0}{3\epsilon_s}\left(\frac{\sigma_{\mathrm{e}}(0)}{s_0 g(\varphi_c)}\right)^n. \tag{57}$$

To proceed further, a specific expression for $\sigma_{\mathrm{e}}(0)$ is required which is obtainable from Eq. (53) as

$$\sigma_{\mathrm{e}}(0) = -\left(\frac{1+\nu}{1-\nu}\right)\mu\left(\frac{D\dot{\epsilon}_0}{V^2}\right)I + 6\epsilon_s\varphi_c\mu\left(\frac{1+\nu}{1-\nu}\right), \tag{58}$$

where

$$I \equiv \int_0^\infty \left(\frac{\eta}{g(\varphi)}\right)^n \mathrm{d}\zeta \tag{59}$$

is a definite integral, which combines all of the most non-linear effects in the total strain rate expressions. We will refer to it as the *dissipation integral*. As the integral contains in its integrand $\sigma_{\mathrm{e}}(\zeta)$ which is not known without obtaining the simultaneous solutions of Eqs. (51) and (52), it cannot be evaluated exactly. If, however, the two-coupled equations could be solved, then the evaluation of the dissipation integral would contribute only a pure number to the overall expression for the case II front velocity. Therefore, we approximate the solution of the integral by assuming that the dependence of $\sigma_{\mathrm{e}}$ on $\zeta$ in the Fickian domain must resemble that of the diluent concentration $\varphi$ ($\zeta$) itself, i.e. it is likely to be close to

$$\sigma_{\mathrm{e}}(\zeta) = \sigma'_{\mathrm{e}}(0)\exp(-\zeta), \tag{60}$$

where $\sigma'_{\mathrm{e}}(0)$ is taken to be equal to that given for the case of the abrupt e–p transition expression of Eq. (42). Then, a reasonably close expression for the dissipation integral would become,

$$I \approx \left(\frac{6\epsilon_s\varphi_c\mu(1+\nu)}{s_0(1-\nu)}\right)^n \int_0^\infty \exp[mn\varphi_c\exp(-\zeta) - n\zeta]\,\mathrm{d}\zeta. \tag{61}$$

With these modifications the case II front velocity in the model of a gradual e–p transition becomes

$$V = \sqrt{\frac{2\nu}{(1-\nu)}\left(\frac{D\dot{\epsilon}_0(T)\mu}{s_0 g(\varphi_c)}\right)\left(\frac{6(1+\nu)}{(1-\nu)}\frac{\epsilon_s\varphi_c\mu}{s_0 g(\varphi_c)}\right)^{n-1}\left[1 - \frac{1}{6\epsilon_s\varphi_c}\left(\frac{D\dot{\epsilon}_0}{V^2}\right)I\right]^n}. \tag{62}$$

We note that Eq. (62) incorporating inelastic relaxation inside the Fickian field and Eq. (48) without inelastic relaxation differ by a factor of

$$\left\{\frac{\nu}{(1-\nu)}\left[1 - \frac{1}{6\epsilon_s\varphi_c}\frac{D\dot{\epsilon}_0}{V^2}I\right]^n\right\}^{1/2}, \tag{63}$$

which is always less than unity indicating that with inelastic relaxations inside the Fickian zone the case II front will advance slower.

### *2.9. Case II front velocity in models with an out-of-surface tensile stress present*

Referring back to the findings of Section 2.3 and Eqs. (28a) and (29a), we proceed as in Sections 2.6 and 2.8 to develop expressions for the case II front velocity where an out-of-surface tensile stress $\sigma_{11}$ is present for the two models of abrupt e–p transition and gradual e–p transition. As noted earlier, Eqs. (28a) and (29a) are identical with Eqs. (21a) and (22a) for the case where $\sigma_{11} = 0$. The only difference that separates the two developments is that the effective stress $\sigma_{\mathrm{e}}$ is different in the present case, as given by Eq. (25). With this straightforward modification the two corresponding expressions become

$$V = \sqrt{\left(\frac{1-\nu}{1+\nu}\right)\frac{\dot{\epsilon}_0 D}{3\epsilon_s\varphi_c}\left[\frac{\sigma_{11} + 6\epsilon_s\varphi_c\mu(1+\nu)/(1-\nu)}{s_0 g(\varphi_c)}\right]^n} \tag{64}$$

for the abrupt e–p transition and

$$V = \sqrt{\left(\frac{\nu}{1+\nu}\right)\frac{\dot{\epsilon}_0 D}{3\epsilon_s\varphi_c}\left[\frac{\sigma_{11} + 6\epsilon_s\varphi_c\mu(1+\nu)/(1-\nu) - (1+\nu)/(1-\nu)((\dot{\epsilon}_0 D)/(V^2))\mu I'}{s_0 g(\varphi_c)}\right]^n} \tag{65}$$

for the gradual e–p transition, where

$$I' \equiv \int_0^\infty \left(\frac{\sigma_{11}}{s_0} + \frac{6\epsilon_s\varphi_c\mu(1+\nu)/(1-\nu)}{s_0}\exp(-\zeta)\right)^n \times \exp(mn\varphi_c\exp(-\zeta))\,d\zeta \tag{66}$$

is a modified dissipation integral, which is identical to that of Eq. (61) when $\sigma_{11} \to 0$.

### 2.10. Case II front velocities in normalized form

While Eqs. (48), (62), (64) and (65) are useful in comparing the model predictions with the experiments, more general observations on the case II sorption rates are more readily achieved by introducing normalized relations as far as possible. Moreover, in doing so we introduce also the results for the border conditions discussed in Section 2.5 that relate the case II front velocities directly to the overall chemical potential driving forces given by the external equilibrium diluent concentrations $\varphi_e$.

We note that the case II front velocities are governed by two separate kinetics, that of diffusion, and that of visco-plastic relaxation, characterized by $D(T)$ and $\dot{\epsilon}_0(T)$. With these we define a velocity normalization factor $V_0$.

$$V_0 \equiv \sqrt{\dot{\epsilon}_0(T)D(T)}. \tag{67}$$

The case II front velocity, however, also enters in the border condition between the diluent-enriched glassy polymer and the swollen gel, in the flux continuity across the process zone through the factor $\Lambda V/D$. This we deal with by introducing a factor $\beta$ that is also temperature dependent, albeit much less so than $V_0$, i.e.

$$\frac{\Lambda V}{D} = \frac{V}{V_0}\sqrt{\frac{\dot{\epsilon}(T)}{D(T)}} = \beta\left(\frac{V}{V_0}\right)$$

giving

$$\beta(T) = \Lambda\sqrt{\frac{\dot{\epsilon}_0(T)}{D(T)}}. \tag{68}$$

Moreover, the diluent misfit parameter $\epsilon_s$ enters the expressions repeatedly, making it meaningful introducing a modified misfit parameter.

$$B \equiv \frac{6\epsilon_s\mu}{s_0}\left(\frac{1+\nu}{1-\nu}\right). \tag{69}$$

With these consolidations, we now introduce normalized front velocities as follows:

$$\frac{V}{V_0} = \sqrt{\left(\frac{2\mu}{s_0}\right)\exp\left\{m\varphi_e/\left(1+\beta\frac{V}{V_0}\right)\right\}\left[\frac{B\varphi_e}{(1+\beta(V/V_0))}\exp\left\{m\varphi_e/\left(1+\beta\frac{V}{V_0}\right)\right\}\right]^{n-1}} \tag{70}$$

for the abrupt e–p transition model with $\sigma_{11} = 0$; and

$$\frac{V}{V_0} = \sqrt{A\exp\left\{m\varphi_e/\left(1+\beta\frac{V}{V_0}\right)\right\}\left[\frac{B\varphi_e}{(1+\beta(V/V_0))}\exp\left\{m\varphi_e/\left(1+\beta\frac{V}{V_0}\right)\right\}\right]^{n-1}\times G}, \tag{71a}$$

where

$$A = \frac{2\nu}{(1-\nu)}\frac{\mu}{s_0}, \tag{71b}$$

$$G = \left\{1 - \left(\frac{V_0}{V}\right)^2\frac{(1+\beta(V/V_0))}{6\varphi_e\epsilon_s}I(\varphi_e)\right\}^n, \tag{71c}$$

with

$$I \equiv \left(\frac{B\varphi_e}{((1+\beta(V/V_0)))}\right)^n \times \int_0^\infty \exp\left\{n\left[\frac{m\varphi_e}{(1+\beta(V/V_0))}\exp(-\zeta) - \zeta\right]\right\}d\zeta \tag{71d}$$

for the gradual e–p transition model with $\sigma_{11} = 0$.

For the cases where $\sigma_{11}$ is present,

$$\frac{V}{V_0} = \sqrt{\frac{2\mu}{s_0}\frac{(1+\beta(V/V_0))}{B\varphi_e}\left[\frac{\sigma_{11}}{s_0} + \frac{B\varphi_e}{(1+\beta(V/V_0))}\right]^n\exp nm\varphi_e/\left(1+\beta\frac{V}{V_0}\right)} \tag{72}$$

for the abrupt e–p transition model and

$$\frac{V}{V_0} = \sqrt{\frac{A(1+\beta(V/V_0))}{B\varphi_e}\left[\frac{\sigma_{11}}{s_0} + \frac{B\varphi_e}{(1+\beta(V/V_0))} - \frac{B}{6\epsilon_s}\left(\frac{V_0}{V}\right)^2 I'\right]^n\exp\left\{nm\varphi_e/\left(1+\beta\frac{V}{V_0}\right)\right\}}, \tag{73a}$$

Table 1
Diffusion constants, misfit parameters, values for $V_0$ and $\beta$ for the three chosen Iodoalkane diluents at room temperature

| Diluent type | $D(cm^2/s)$[a] | $\epsilon_3$[b] | $V_0$ (nm/s)[c] | $\beta$[d] |
|---|---|---|---|---|
| $C_5H_{11}$ I | $3.0 \times 10^{-13}$ | $5.53 \times 10^{-3}$ | 10.54 | 158 |
| $C_6H_{13}$ I | $1.0 \times 10^{-13}$ | $5.88 \times 10^{-3}$ | 6.09 | 274 |
| $C_8H_{17}$ I | $3.5 \times 10^{-15}$ | $6.27 \times 10^{-3}$ | 1.14 | 1463 |

[a] From Gall et al. [6].
[b] Re-scaled from the $C_6H_{13}I$ estimate, according to the effective molecular diameters reported by Gall et al. [6].
[c] Eq. (67).
[d] Eq. (68).

where

$$I' \equiv \int_0^\infty \left( \frac{\sigma_{11}}{s_0} + \frac{B\varphi_e}{(1+\beta(V/V_0))} \exp(-\zeta) \right)^n \times \exp\left\{ \left( nm\varphi_e / \left( 1 + \beta \frac{V}{V_0} \right) \right) \exp(-\zeta) \right\} d\zeta \tag{73b}$$

for the graduated e–p transition model.

## 3. Model predictions

### 3.1. Tuning-in the model

As stated earlier, the case II sorption process is complex in its synergistic interactions between chemical potential governed driving forces, diffusion of the diluent with its attendant material misfit, the plasticization effects and the elasto-visco-plastic processes initiated in the Fickian diffusion field and the process front. The theoretical model introduced in Section 2 requires a number of material parameters and their interactive alterations. Many of these parameters have not been measured and are difficult to measure uniquely. Therefore, a number of simplifications were made in the model to make it manageable. In this section we will discuss the procedure we have adopted to determine some of the more important parameters from the published diffusion experiments. While our theoretical model is general, we will primarily explore its relation to the series of detailed experiments of Gall et al. [6] of diffusion of iodoalkanes into polystyrene, but will also utilize the experiments of Gall and Kramer [5], and Lasky et al. [4].

The experiment of Lasky et al. [4] and those of Gall et al. [6] on the initiation of motion of a case II sorption front in polystyrene with iodohexane provide an opportunity to evaluate some of the important model parameters.

The "driving force" for the diffusional penetration of a diluent into the surface is the current osmotic suction

$$\Sigma = \frac{RT}{\Omega} \ln \frac{\varphi_e}{\varphi_s}. \tag{4}$$

When $\varphi_s$ at the surface reaches a critical level, $\varphi_c$, the case II front can advance self similarly (subject to the conditions discussed in Section 2.1) where the misfit induced pressure evokes an effective stress $\sigma_e$ that reaches the plastic resistance of the diluent-enriched polymer. As discussed in Section 2.1 the sorbed misfitting diluent molecules in the Fickian precursor field will set up a pressure $p$ that counteracts the osmotic suction. If the condition of $\Sigma - p = 0$ is reached before $\varphi_s$ reaches $\varphi_c$, the misfit-induced pressure in the surface layer will reach the full level of an osmotic pressure $\Pi$ to stall the case II front. This pressure is given by

$$p = \frac{4\mu(1+\nu)}{(1-\nu)} \epsilon_s \varphi, \tag{74}$$

for any local diluent concentration $\varphi$, where all terms are as defined in Section 2. It reaches its maximum value at the free surface in a stationary diffusion front. We estimate the spherical equivalent molecular volume, $\Omega$, of iodohexane as

$$\Omega = \frac{M_w}{\rho} \tag{75}$$

for any local diluent concentration $\varphi$, where $M_w = 208$ g/mol is its molecular weight and $\rho = 1.52$ g/cm$^3$ its estimated density, giving $\Omega = 1.37 \times 10^{-4}$ m$^3$/mol. We now consider the experiment of Lasky et al. [4] where for $\varphi_e = 0.083$, $\varphi_s = 0.07$ and the case II front never moved after an appropriate Fickian precursor was observed to form. Thus, we conclude that $\Sigma - p \leq 0$ and from Eqs.(4), (74) and (75) we estimate that

$$\epsilon_s \geq \frac{RT}{4\Omega\varphi_e\mu} \frac{(1-\nu)}{(1+\nu)} \left( \frac{\varphi_e}{\varphi_s} \ln \frac{\varphi_e}{\varphi_s} \right) = 5.88 \times 10^{-3} \tag{76}$$

for $\mu = 1.0$ GPa, $\nu = 0.3$ at $T = 295$ K for iodohexane in polystyrene.

This gives $p = 3.06$ MPa and an associated effective stress of $\sigma_e = 3/2p = 4.59$ MPa which was apparently insufficient to overcome the plastic resistance of the diluent-enriched surface layers. In a second experiment Lasky et al. [4] have found that when $\varphi_e$ was increased to 0.16 for which $\varphi_s$ reached 0.11, the case II front began to advance. Under these conditions we estimate for the same $\epsilon_s$, a misfit induced maximum pressure of 4.80 MPa in the surface layers with an accompanying effective stress of $\sigma_e = 7.21$ MPa. This now apparently equals, or exceeds to some extent, the effective tensile plastic resistance $Y$ of the diluent-enriched surface layers. As at room temperature the tensile plastic resistance $Y_0$ of pure polystyrene is around 80 MPa, and the temperature dependence of the plastic relaxation of the unmodified polymer and the diluent-enriched one will be assumed to be the same, we have

$$\frac{Y}{Y_0} = \frac{s}{s_0} = \exp(-m\varphi_c) \tag{77}$$

giving for this experiment where $\varphi_s = \varphi_c = 0.11$ a plasticization factor of $m = 21.9$. This represents a dramatic reduction of the plastic resistance of PS due to sorption of iodohexane to a concentration of $\varphi_c = 0.11$. In the absence

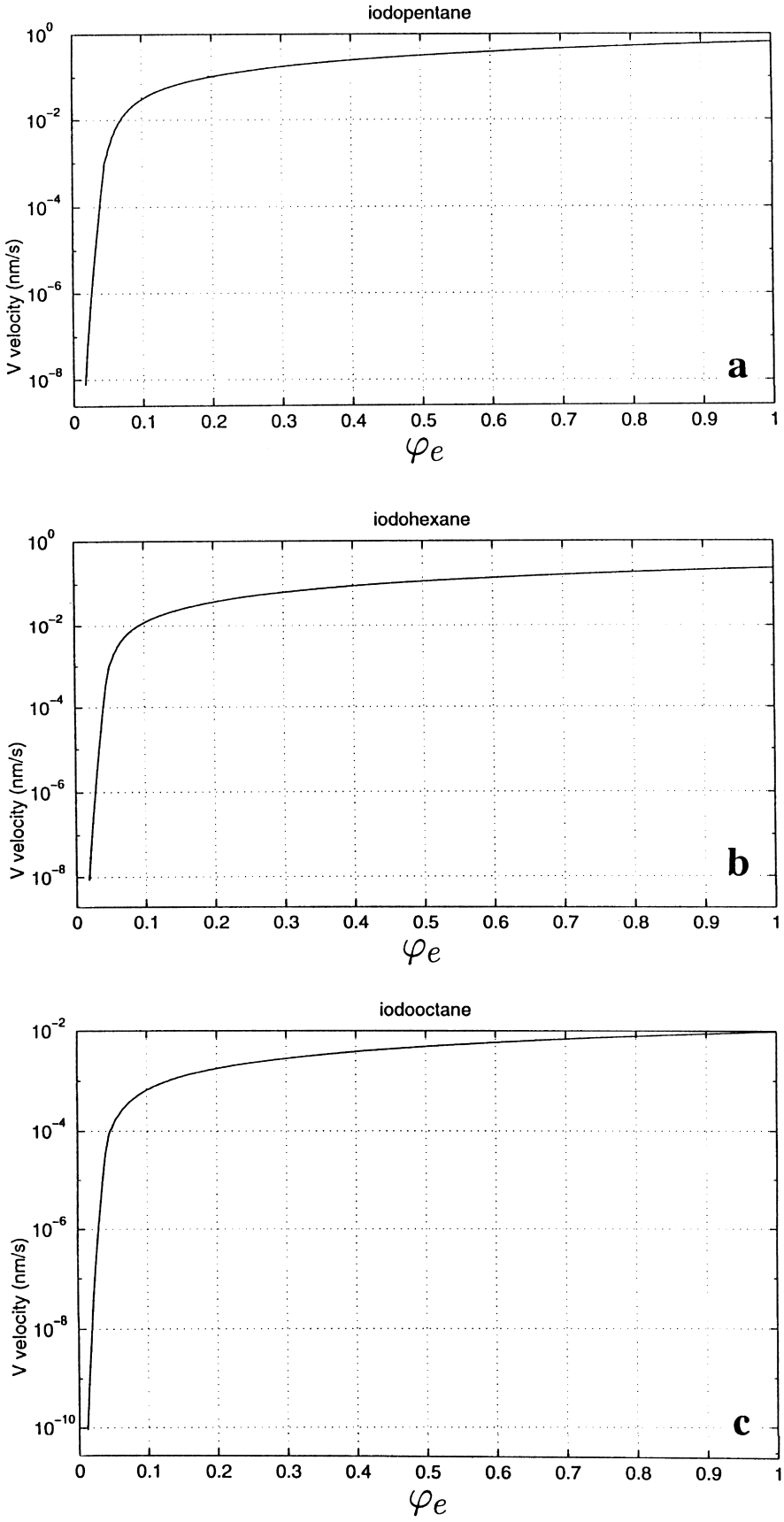


Fig. 3. Calculated dependence of the case II front velocity on external diluent concentration for three iodoalkanes penetrating into polystyrene: (a) iodopentane; (b) iodohexane; (c) iodooctane, all at room temperature, for an abrupt e–p transition at the process front.

of more precise information we consider these estimates based on the behavior of the iodohexane/PS system as useful base values to estimate the corresponding model parameters for the other iodoalkanes considered by Gall et al. [6]. In our model predictions developed in the following sections, however, we will limit our comparisons to only iodopentane, iodohexane and iodooctane.

For the specific predictions of the aforementioned three iodoalkanes we choose the following material parameters for polystyrene at room temperature.

$\mu = 1.00$ GPa
$\nu = 0.3$
$m = 21.9$
$\Lambda = 4.5 \times 10^{-5}$ cm (Section 2.5)
$s_0 = 238$ MPa (Appendix A)
$\dot{\epsilon}_0(T) = 3.70\ s^{-1}$ (Appendix A)
$n = 7.8$ (Appendix A)

The diffusion constants $D$ and the re-scaled misfit parameter $\epsilon_s$ for the three chosen iodoalkanes are listed in Table 1.

In the following sections we will first determine the dependence of case II front velocities in polystyrene at room temperature on the external equilibrium concentration of the three selected iodoalkanes, driven only by material misfit. We will perform this evaluation first for the idealized model with an abrupt e–p transition in non-normalized form to permit a direct comparison with the measurements of Gall et al. [6]. In a subsequent section we will repeat this evaluation in normalized form and follow it with another normalized form evaluation of the model employing a gradual e–p transition. In the normalized form the models permit ready scaling of the case II front penetration at different temperatures, affecting both the diffusion constant $D$ and the visco-plastic rate constant $\dot{\epsilon}_0(T)$ through the normalization velocity $V_0$. Following these, we then perform evaluations of the kinetics of case II front motion, in normalized form, for three levels of out-of-surface tensile stress, $\sigma_{11}$, but only for the model with the gradual e–p transition, and then only for the case of iodohexane, as a demonstration case.

### 3.2. Case II front propagating by diluent induced material misfit alone

#### 3.2.1. Idealized model of abrupt visco-plastic transition at case II front

The case II front velocity in this idealized model is given by Eq. (48), which we present later in a fully detailed form as,

$$V = \sqrt{\frac{2\mu\dot{\epsilon}_0(T)D}{s_0}\exp\{m\varphi_e/(1+\Lambda V/D)\}\left[\frac{B\varphi_e}{(1+\Lambda V/D)}\exp\{m\varphi_e/(1+\Lambda V/D)\}\right]^{n-1}}, \tag{48a}$$

where $B$ is as defined by Eq. (69). The values of the diluent and material parameters to be used for the evaluation at room temperature were listed earlier. Of interest is the form of the relation $V = V(\varphi_e)$ for the three selected iodoalkanes. Clearly, the solution of Eq. (48a) for $V$, for a given $\varphi_e$ requires a numerical procedure as the unknown dependent parameter $V$ appears on both sides of the equation. For small concentrations $\varphi_e$ leading to small velocities the term $\Lambda V/D$ contributes only a negligible effect, and the evaluation can be carried out explicitly. This will be the anomolous diffusion region where $\varphi_c \leq \varphi_e$. However, when velocities become larger in the case II range where $\varphi_c < \varphi_e$, and the difference increases, the $\Lambda V/D$ term begins to make significant contributions.

The calculated dependence $V = V(\varphi_e)$ for iodopentane, iodohexane and iodooctane are given in Fig. 3(a)–(c). The figures show a continuous behavior consisting of two branches. The case II diffusion-sorption branch for external equilibrium diluent concentrations exceeding $\varphi_e \approx 0.1$, and a second branch of steeply decreasing velocities with decreasing $\varphi_e < 0.1$. This second branch that has been termed *anomolous diffusion* is not different in character from the case II diffusion-sorption branch, and has nothing anomolous in its character but results simply from the steep decline of the visco-plastic constitutive connection between effective inelastic strain rate $\dot{\epsilon}_e^p$ and effective stress $\sigma_e$ given by Eq. (12). We note, however, that as $\varphi_e$ decreases into the few percentile range the entire model with its idealized behavior of the diluent-enriched glassy polymer may no longer be reliable, particularly for cases where the levels of $\varphi_e$ are below what would be required for a glass to gel transition. Similar departures from reality must be expected for $\varphi_e$ approaching unity.

In Fig. 4(a)–(c) we present the same results of Fig. 3(a)–(c) in normalized form through the use of Eq. (70). In this form of representation the changed behavior of the case II front at different temperatures can be gleaned by re-scaling the results according to the temperature dependence of the velocity normalization factor $V_0$ which brings in the most important temperature effect, coming in through the temperature dependence of the visco-plastic strain rate pre-factor $\dot{\epsilon}_0(T)$ of the glassy polymer and the temperature dependence of the diffusion constant $D$. Other temperature dependent factors such as $\beta$ and the exponent $n$ cannot be readily re-scaled and are taken as constants as a first approximation.

#### 3.2.2. Model with gradual elastic-to-plastic transition

The behavior of the case II front in this more realistic representation, accounting for visco-plastic relaxations in the entire Fickian diffusion misfit front, is evaluated in normalized form according to Eqs. (71a)–(71c) using the previously presented material parameters and those listed in Table 1.

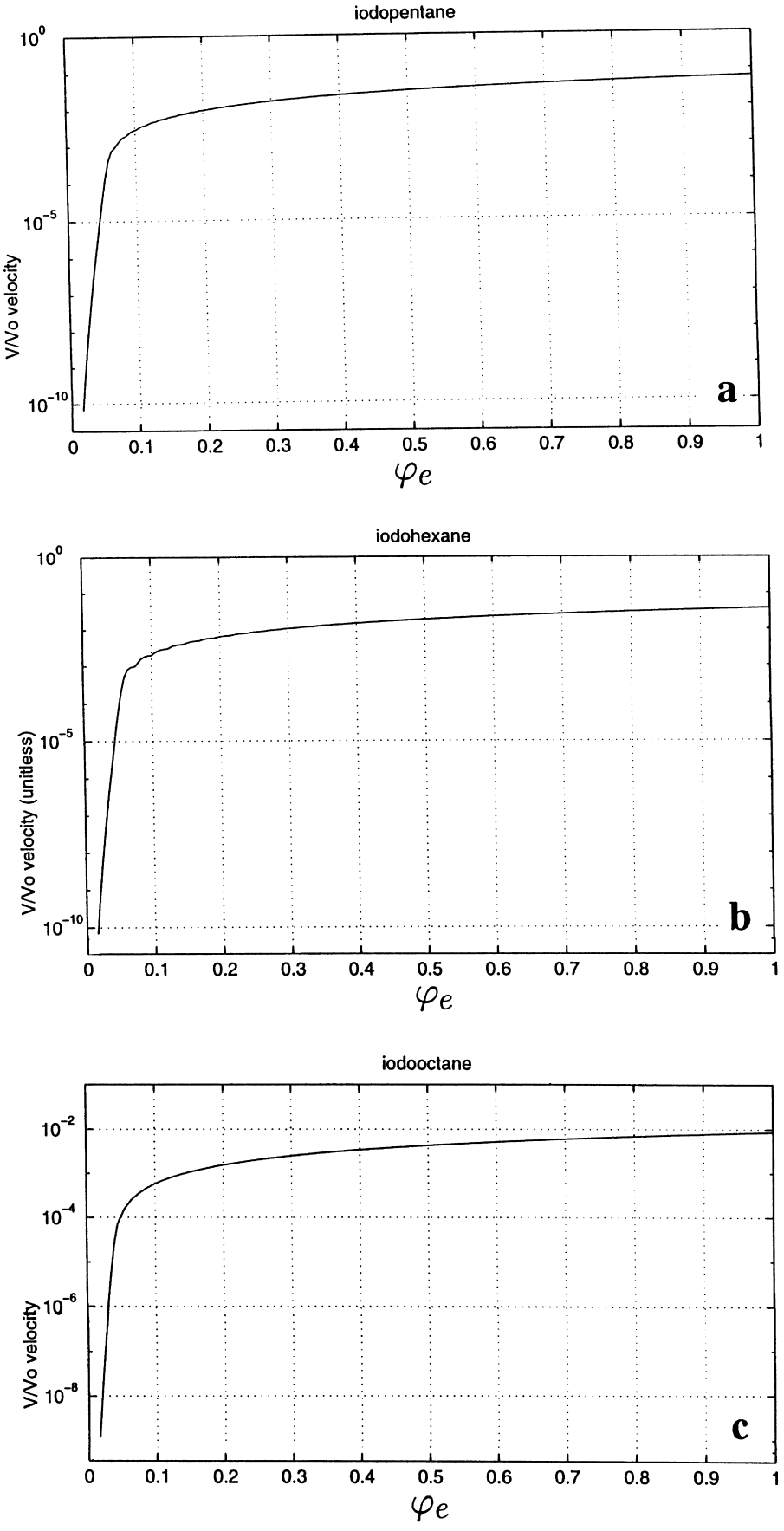


Fig. 4. Calculated normalized dependence $V/V_0$ on $\vartheta_e$ for the same iodoalkanes given in Fig. 3: (a) iodopentane; (b) iodohexane; (c) iodooctane.

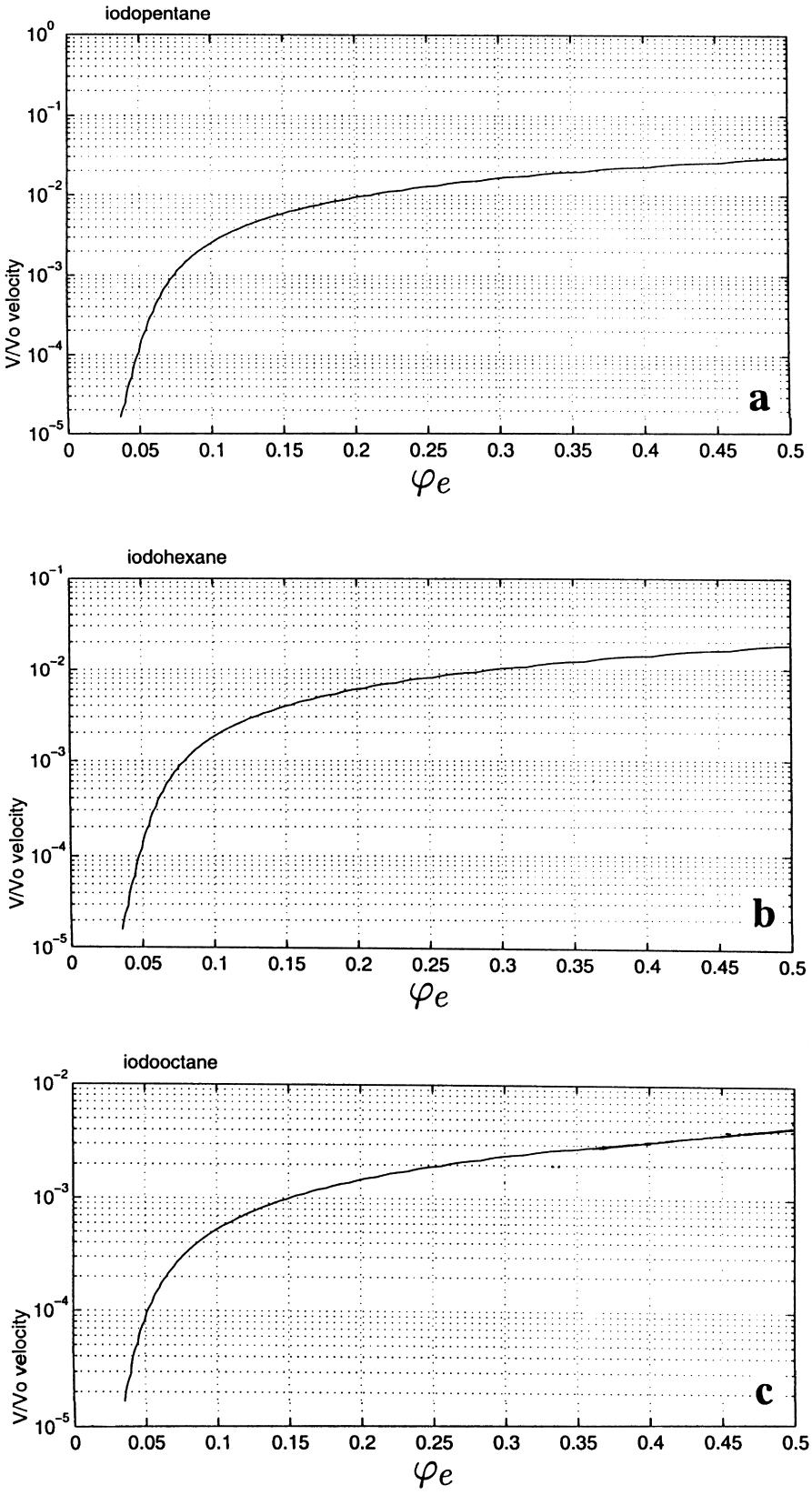


Fig. 5. Calculated normalized dependence of $V/V_0$ on $\varphi_e$ for three iodoalkanes into polystyrene at room temperature in a model with a gradual e–p transition: (a) iodopentane; (b) iodohexane, (c) iodooctane.

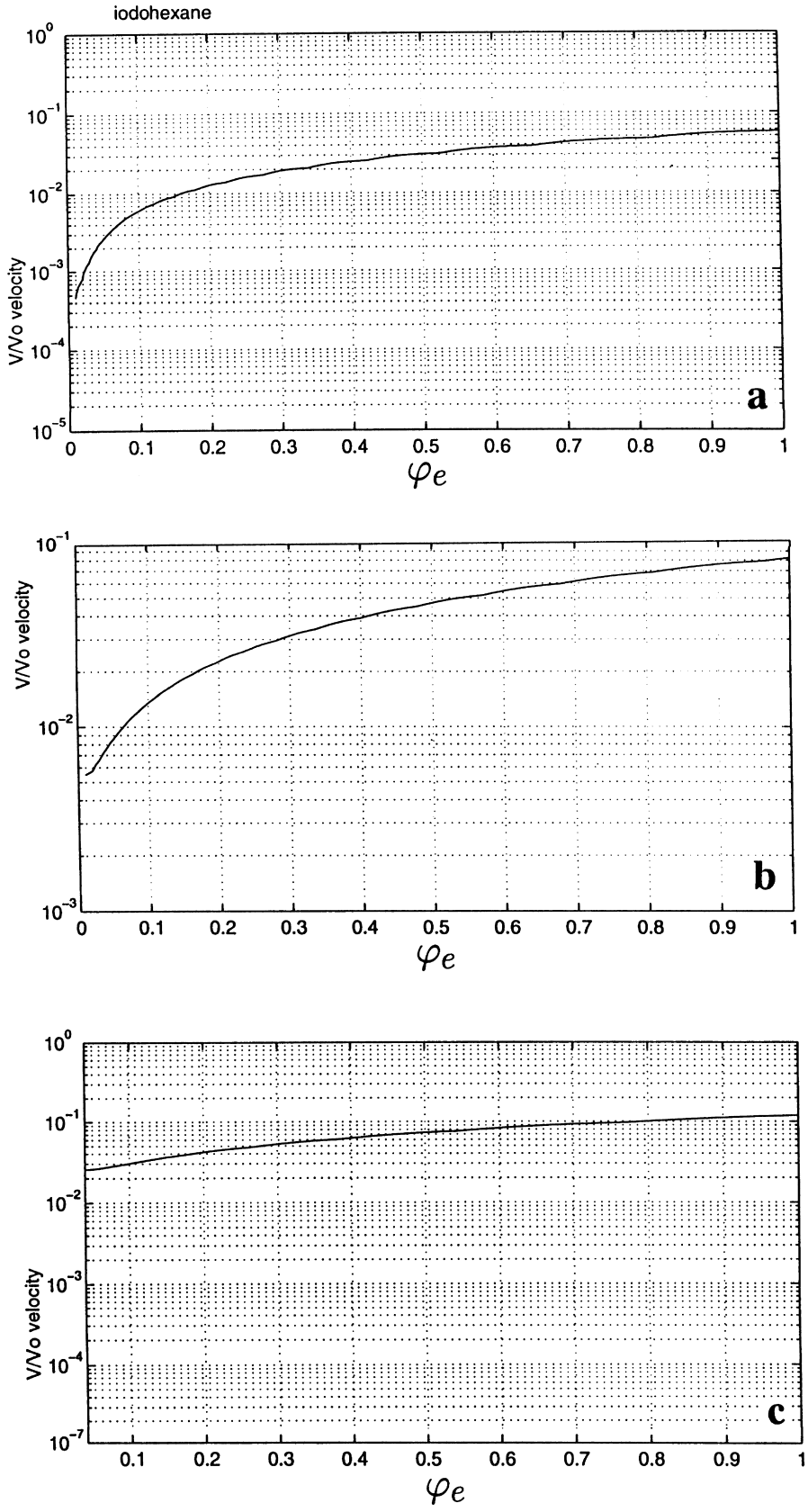


Fig. 6. Calculated normalized dependence of $V/V_0$ on $\varphi_e$ for iodohexane into polystyrene at room temperature in a model with a gradual e–p transition for three levels of out-of-surface tensile stress (in units of $s_0$): (a) $\sigma_{11}/s_0 = 4.2 \times 10^{-2}$; (b) $\sigma_{11}/s_0 = 8.4 \times 10^{-2}$; (c) $\sigma_{11}/s_0 = 12.6 \times 10^{-2}$.

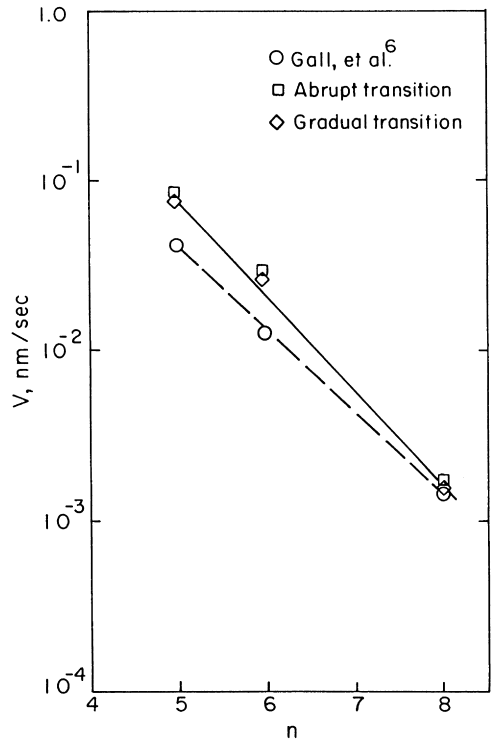


Fig. 7. Comparison of model predictions for case II front velocity $V$ into polystyrene on number of carbon atoms n in iodoalkanes at room temperature for a common surface diluent activity level of $a = 0.45$, based on a model with a sharp e–p transition (□) and on a model with a gradual elastic to plastic transition (◇). Experimental measurements of Gall et al. [6] (○) are shown for comparison.

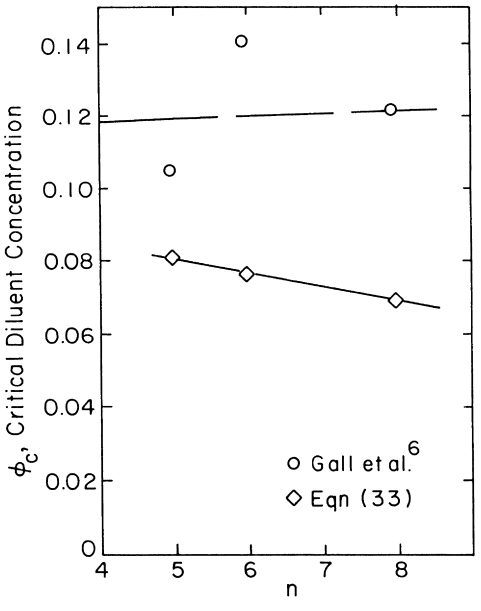


Fig. 8. Calculated dependence of critical diluent concentrations $\varphi_c$ at the case II process front on the number of carbon atoms in the iodoalkanes based on the gradual e–p transition (◇). Experimental measurements of Gall et al. [6] (○) are shown for comparison.

The results are presented in Fig. 5(a)–(c). Comparison of these results with those of Fig. 4(a)–(c) for the case of the abrupt elastic to plastic transition show very similar behavior but a somewhat reduced velocity for the same external diluent concentration as was expected from Eq. (63). We will consider this effect in more detail in Section 4 discussing the quality of our findings.

### *3.3. Case II front propagating under the combined action of the diluent induced material misfit and an out-of-surface tensile stress $\sigma_{11}$*

As discussed in Section 2.3, the presence of a tensile stress acting across the plane of the case II sorption front will significantly elevate the effective stress $\sigma_e$ in the Fickian field of diffusion and accelerate visco-plastic flow. This effect was evaluated in Section 2.9 for both the simplified model of an abrupt e–p transition given by Eq. (64) and for the model with a gradual e–p transition given by Eqs. (65) and (66). Here we evaluate this effect in normalized form for only the model with the gradual e–p transition at three levels of $\sigma_{11}/s_0$ of $4.2 \times 10^{-2}$, $8.4 \times 10^{-2}$ and $12.6 \times 10^{-2}$, and only for the case of iodohexane.

Fig. 6(a)–(c) give the dependence of the case II front velocity in normalized form on $\varphi_e$ in the model with the gradual e–p transition for the three stress levels stated earlier for iodohexane, based on Eqs. (73a) and (73b).

## 4. Discussion

### *4.1. Comparison with experiments*

In several areas meaningful comparisons can be made between model predictions and experimental measurements of Gall et al. [6]. The first of such comparisons is the case II front velocity for an external activity level of $a = 0.45$ ($\varphi_e = 0.203$) used by Gall et al. in all of their diluent penetration experiments. First, we note that the diluent concentration $\varphi_e$ in the gel behind the case II front, reported by these authors, is less than what is imposed by the external environment, but is progressively rising to the externally imposed concentration. For the case of iodopentane (Fig. 3 of Ref. [6]) $\varphi_e$ in the gel is given as 0.18. This indicates that the gel offers a transient resistance to swelling which is likely to be a result of molecular entanglements in the gel. Thus, in our evaluations we will take $\varphi_e$ in the gel to be 0.18 for all cases.

In Fig. 7 we show the predicted case II front velocities for the three chosen iodoalkanes, as determined from Fig. 4(a)–(c) for the abrupt e–p transition model (□) and from Fig. 5(a)–(c) for the gradual e–p transition model (◇), using the $V_0$ values listed in Table 1. We note first that while the velocities calculated from the gradual e–p transition model are indeed somewhat lower than those calculated from the abrupt e–p transition model, the differences are small and do not warrant using the much more complex gradual transition model in general. Fig. 7 shows also the

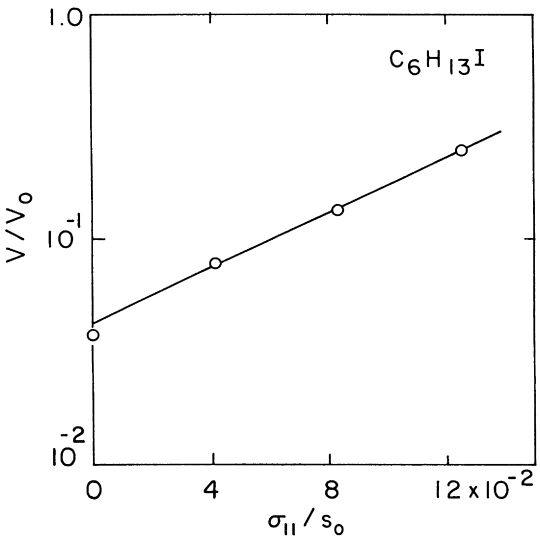


Fig. 9. Dependence of the calculated normalized case II front velocity $V/V_0$ on the level of the out-of-surface tensile stress $\sigma_{11}/s_0$ for iodohexane into polystyrene at room temperature based on the gradual e–p transition model, for a diluent surface activity level of $a = 0.45$.

three corresponding experimental measurements of Gall et al. [6] (○). The model predictions are consistently higher than the experimental measurements. Moreover, the rate of change of the velocity with increasing numbers of carbon atoms in the diluents is also steeper. Nevertheless, considering the sparse nature of available material information and the various necessary idealizations and approximations made in the model, the agreement is considered to be quite satisfactory.

Another comparison that can be made is for the critical diluent concentration $\varphi_c$ required for the motion of the case II front and its dependence on the number of carbon atoms in the diluents. This dependence is obtainable from Eq. (33) stating the border condition of diluent flux continuity. The resulting dependence is shown in Fig. 8 with the diamonds (◇) and indicates a slight decrease of $\varphi_c$ with $n$ on the argument that the larger iodoalkane molecules must have a somewhat larger effective molecular diameter and are associated with a larger misfit parameter. The actual measurements of Gall et al. for these three chosen diluents are also shown as the circular points together with their "best fit" line based on the measured $\varphi_c$ concentrations of other iodoalkanes. Apart from the large scatter in the experimental measurements they lie considerably above our predictions. Examination of the structure of Eq. (33) gives the reason. For a fixed $\beta$ coefficient an over prediction in the normalized velocity $V/V_0$ will give an under prediction for $\varphi_c$. As the entire model is fully interconnected, it is difficult to identify a single cause, which gives over estimates of $V/V_0$ and associated underestimates of $\varphi_c$. Clearly, a systematic variation in the chosen balances of the parameters $\epsilon_s$, $m$, and $\Lambda$ could have given better overall agreement. As this would not shed any further insight into the process, it was not done.

In another comparison with the measurements there is a major difference between our model and their findings. In

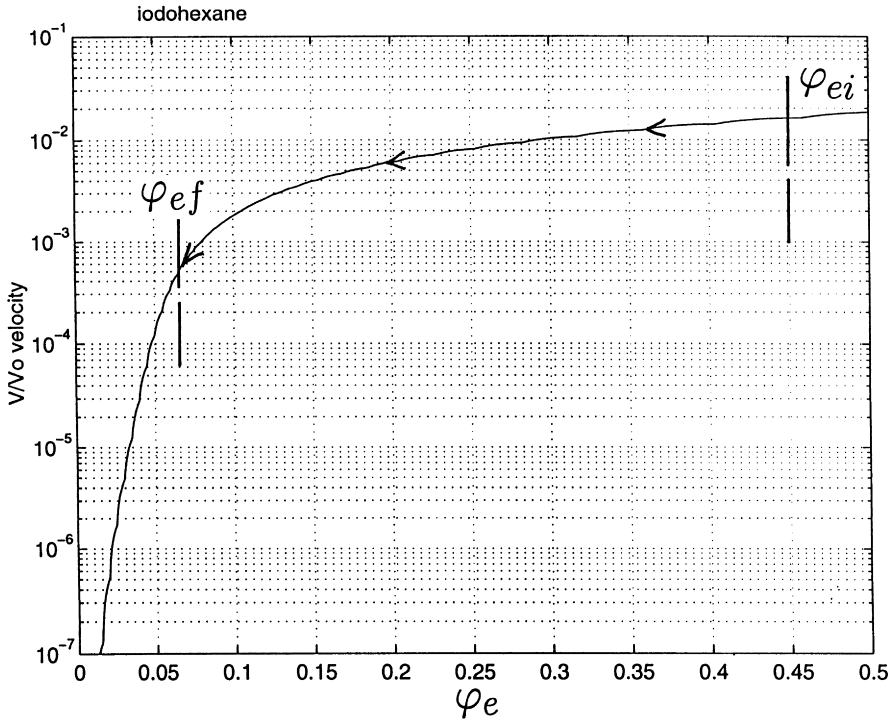


Fig. 10. Schematic representation of conditions in the limited (diluent) supply diffusion experiments of Nealey et al. [18] utilizing RDP diffusing into ULTEM.

Fig. 10 of Gall et al. the authors report the rate of increase in surface diluent concentration (which they incorrectly label as swelling rate)[4] at the onset of case II front motion, and find that this rate decreases by three orders of magnitude between iodopropane ($n = 3$) and iodooctane ($n = 8$). In our model based on the self similar advance of the case II front this same rate of increase, given by our Eq. (47) is shown to be dependent primarily on the visco-plastic rate coefficient $\dot{\epsilon}_0(T)$ and the misfit parameters $\epsilon_s$ of the diluents, which show only a mild dependence on the diluent character over the entire range of $n$ of the alkanes as shown in Table 1 (based on our method of a re-scaling of these parameters from the fit obtained to iodohexane). The apparent conflict is resolved if it is noted that Gall et al. have based their measurements on the rate of change of surface diluent concentration in the *stationary* Fickian pre-cursor, prior to case II front motion. In this range of behavior where visco-plastic relaxations are of little consequence (as we have discussed earlier by comparing the results of the abrupt e–p transitions to the gradual e–p transitions) the rate of change of surface diluent concentration should be given by Fick's law. Then, contrary to the assertions of the authors $\dot{\varphi}$ should indeed reflect directly a dependence on the diffusion constant, which explains the large decreases of $\dot{\varphi}$ with increasing $n$. That this is so can be verified directly by evaluating $\dot{\varphi}/D$ in their measurements which is substantially constant over the range of $n$ within the scatter of the measurements shown in Fig. 10 of Ref [6]. In contrast, our developments are based on the propagation of a case II front in a self-similar form, with an attached Fickian precursor of diluent concentration. Thus we are convinced that the conflict is entirely based on this difference between a stationary front and a moving one.

### 4.2. Effect of an out-of-surface tensile stress on the case II front velocity

The important effect of a sustained out-of-surface tensile stress $\sigma_{11}$ as evaluated in Section 3.3 and shown in Fig. 6(a)–(c) for iodohexane is summarized in Fig. 9 for the same level of activity $a = 0.45$ used in the experiments of Gall et al. [6]. The figure indicates that the effect is exponential and monotonic in the range investigated. For a stress level $\sigma_{11}/s_0 = 12.6 \times 10^{-2} (= 30$ MPa) there is an increase in the case II front velocity by a factor of about 6.5 in comparison with the unstressed case. The importance of this effect on solvent crazing was first pointed out by Brown [17]. Other stress dependences in the case II sorption process had been considered earlier, starting with the TW model that had introduced the notion of increased diluent solubility in the presence of a negative pressure [2]. This effect that had been incorporated into the diluent toughening model of Argon et al. [16] has been difficult to verify. Thus, in the experiments of Nealey et al. [18] studying the case II diffusion of RDP (resorcinol bis(diphenyl-phosphate)) into Ultem (poly(ether-imide)) ring-on-ring bi-axial bending experiments were performed in association with the case II sorption measurements where both tensile and compressive bi-axial stresses were applied to the thin disks of Ultem subjected to RDP penetration. No important effect of the bending stress was observable. While the reason for this failure was not clear, it is likely that the bi-axial stresses in the outer elements of the bent disks might have undergone substantial inelastic relaxation. The case of the out-of-surface tensile stress present at the base of craze tufts would be different, as the stress would be sustained for as long as the craze supports a tensile stress. This effect has been incorporated now in a new model of crazing of diluent toughened polymers [27].

### 4.3. Limited supply case II diffusion

To more closely parallel the conditions of the pre-packaged diluent induced toughening mechanism explored by Gebizlioglu, et al. [19] Nealey, et al. [18] carried out experiments of case II diffusion in which a limited supply of diluent was applied to the surface of a glassy polymer resulting in a gradually decreasing rate of penetration of a case II front into the glassy polymer as the equilibrium diluent concentration in the rubbery gel monotonically droped from some initial level $\varphi_{ei}$ to a final level $\varphi_{ef}$ where the case II front stalled. At the final condition when the front stalls the total diluent content in the entire swollen gel zone behind the case II front contains the same total diluent content applied to the surface at the higher concentration $\varphi_{ei}$. The many interesting and revealing aspects of this complex experiment have been discussed in detail by Nealey et al. Our present case II sorption model can provide considerable insight into this special diffusion scenario, if it can be assumed that the entire transient process of the decelerating diffusion front can be treated as a succession of steady state processes of front penetration in response to the current diluent concentration in the rubbery gel behind the front. However the Nealey experiments provide a certain cut-off to the case II front behavior represented in Figs. 4–6.

Thus, consider, e.g. the schematic dependence of $V/V_0$ on $\varphi_e$ shown in Fig. 10, using results for iodohexane given in Fig. 5(b) as a generic representation of the case II front behavior of RDP diffusing into Ultem. If $\varphi_{ei}$ represents the initial diluent concentration applied to the free surface, the RDP will penetrate into the glassy Ultem at an initial velocity $V_i/V_0$ after the usual incubation time required to establish a Fickian precursor. Under the constraint of a limited supply of diluent, however, as further front penetration occurs $\varphi_e$ decreases down the curve of $V/V_0$ as depicted in the figure. Nealey et al. noted that the case II front eventually stalls altogether when at the temperature of the

[4] As we point out in our development, in the constrained penetration of the diluent in the Fickian precursor field the actual swelling rate is given by $\dot{\epsilon}_{11}$ since $\dot{\epsilon}_{22} = \dot{\epsilon}_{33} = 0$.

experiment $\varphi_e$ decreased to a critical level $\varphi_{ef}$ where the rubbery gel behind the case II front underwent a glass transition into a glassy state itself. Clearly, under this condition the case II front will stop moving as the material to be extruded out of the case II process zone will encounter a suddenly increased deformation resistance. This important observation indicates that the case II pattern of behavior represented in Figs. 3–6 must be terminated at a definite concentration $\varphi_e$ below which the material behind the front at the temperature of observation is no longer a rubbery gel but becomes a glass with a steeply increased deformation resistance and equally steeply decreased diffusion constant.

### *4.4. Comparison of the present case II diffusion model with other models*

While adopting many of the assumptions and conditions stated by other models of case II diffusion our model stands out by its clear differentiation of the physical processes of the driving forces and resistances to the sorption process. As most of the recent models have been built on the Thomas and Windle [2] model, we make a direct comparison with that model. In the TW model the activity-driven or chemical-potential-driven sorption process is viewed as being driven by an osmotic pressure, and the effect of this "pressure" is considered to be resisted by a material deformation resistance defined as the "viscosity" of the glassy polymer. We make an important distinction by noting that the "driving force" for the diluent penetration is a chemical potential difference which does not produce a real pressure, but can be considered as an osmotic suction, i.e. a virtual negative pressure, drawing the diluent into the glassy polymer. The sorbed diluent in the Fickian precursor field, however, produces significant material misfit and results in the development of a real pressure which with a free surface present, (or a rubbery gel with negligible deformation resistance present) results in a substantial deviatoric stress that can initiate a process of visco-plastic extrusion of diluent-enriched polymer out of the surface (or into the region of the swollen gel). The misfit induced pressure, however, can reach the level of a real "*osmotic pressure*" to exactly counteract the "*osmotic suction*", and can bring the process to a stand-still. Moreover, the deformation resistance is considered to be that of a non-linear visco-plastic response, i.e. the resulting effective inelastic strain rates are a very non-linear function of the effective stress, rather than being the "linear viscosity" of the TW model.

While many of the case II sorption models, starting with that of Crank [28], have recognized that there must be important internal stresses present in the sorption field, associated with the penetrations of the diluent, none of them, to the best of our knowledge, have actually considered the advance of the case II front in detail as a visco-plastic extrusion process as we have done here.

In this framework our model is on a sound mechanistic basis and capable of predicting quantitatively, quite well, most, if not all, of the case II front phenomena.

## 5. Conclusions

We have presented a detailed model of case II Diffusion of diluents into a glassy polymer. The important features of the model are:

It differentiates clearly the driving forces resulting from chemical potential differences from material-misfit-induced pressures that counteract the penetration.

The model produces a framework of development of a visco-plastic material extrusion process, out of the surface, or into a swollen gel behind the case II process front and provides explicit predictions of case II front velocities related to the external diluent activity.

The development of a self-similarly propagating case II diffusion front requires not only overcoming the visco-plastic resistance of the diluent-enriched polymer at the process front but that the material behind the front remains above its glass transition temperature at the externally imposed diluent concentration in the ambient temperature, to offer only a negligible "back stress".

The model considers explicitly the effect of an out-of-surface tensile stress that very significantly accelerates the diluent penetration. This is seen to be an important factor in solvent and diluent induced toughening of brittle glassy polymers by craze plasticity.

## Acknowledgements

The earlier research on toughening that has stimulated the present model had been supported by the NSF/MRL Program under Grant DMR-90-22933 through the Center for Materials Science and Engineering at MIT. The more recent mechanistic formulations have been supported by the MRSEC program of NSF through the award DMR-94-00334. We are grateful to Professor E.J. Kramer of UCSB for providing vigorous discussion of the mechanism of our model and to Professor D.M. Parks of MIT for critical comments on the consistency of the mechanics aspects. Additional comments of Professor P.F. Nealey of the U. Wisconsin on limited supply diffusion are also gratefully acknowledged.

Table 2
Material rate constants for polystyrene for the power-law expression of Eq. (A.2)

| $T$ (K) | $A$ | $\dot{\epsilon}_0(T)$ s$^{-1}$ | $n$ | $\hat{Y}$ (MPa) |
|---|---|---|---|---|
| 253 | $5.42 \times 10^{12}$ | $2.60 \times 10^{-2}$ | 8.82 | 238 |
| 273 | $9.59 \times 10^{11}$ | $4.14 \times 10^{-1}$ | 8.34 | 238 |
| 295 (RT) | $1.50 \times 10^{11}$ | 3.70 | 7.80 | 238 |
| 300 | $9.17 \times 10^{10}$ | 6.50 | 7.68 | 238 |
| 313 | $3.40 \times 10^{10}$ | 21.70 | 7.37 | 238 |

## Appendix A. Conversion of an exponential rate expression into a power law expression

A mechanism-based expression relating the (effective) plastic strain rate $\dot{\epsilon}_e^p$ to the (effective) stress $\sigma_e$ developed earlier by Argon [23] and further expanded by Argon and Bessonov [26] for a glassy polymer states it to be

$$\dot{\epsilon}_e^p = \dot{\epsilon}_{AB} \exp\left[ -\frac{B}{RT}\left(1 - \left(\frac{\sigma_e}{s_0}\right)^{(5/6)}\right)\right], \tag{A.1}$$

where $\dot{\epsilon}_{AB} = 3 \times 10^{12}\ s^{-1}$ is a typical pre-exponential factor, $B = 31.1$ kcal/mol is a scale factor of the activation free energy of a plastic event and $s_0$ the athermal reference resistance given by

$$s_0 = \frac{0.133}{(1-\nu)}\mu = 238\ \text{MPa},$$

where $\mu$ and $\nu$ are the shear modulus and Poisson's ratio, respectively, and $\mu = 1.25$ GPa, and $\nu = 0.3$.

For the purpose of the developments of the case II sorption model a power-law expression is required having the form.

$$\dot{\epsilon}_e^p = \dot{\epsilon}_0(T)\left(\frac{\sigma_e}{s_0}\right)^n = A\dot{\epsilon}_{AB} \exp\left(-\frac{B}{RT}\right)\left(\frac{\sigma_e}{s_0}\right)^n, \tag{A.2}$$

where

$$A = A_0 \exp\left(-\frac{T}{T_0}\right) \tag{A.3}$$

with $A_0 = 1.05 \times 10^{22}$ and $T_0 = 1183$ K arrived at from phenomenological fits. The resulting "best-fit" values for $A, \dot{\epsilon}_0(T)$ and $n$ for polystyrene are given in Table 2 for several temperatures.

## References


[1] Alfrey T, Gurnee EF, Lloyd WG. J Polymer Sci 1966;12:249.
[2] Thomas NL, Windle AH. Polymer 1982;23:529.
[3] Windle AH. In: Comyn J, editor. Polymer permeability, Amsterdam: Elsevier, 1985. pp. 75.
[4] Lasky RC, Kramer EJ, Hui C-Y. Polymer 1988;29:673.
[5] Gall TP, Kramer EJ. Polymer 1991;32:265.
[6] Gall TP, Lasky RC, Kramer EJ. Polymer 1990;31:1491.
[7] Hui C-Y, Wu K-C, Lasky RC, Kramer EJ. J Appl Phys 1987;61:5129.
[8] Hui C-Y, Wu K-C, Lasky RC, Kramer EJ. J Appl Phys 1987;61:5137.
[9] Hui C-Y, Wu K-C, Lasky RC, Kramer EJ. J Electr Packaging 1989;111:68.
[10] Wu JC, Peppas NA. J Polymer Sci (B) Polymer Phys 1993;31:1503.
[11] Rossi G, Pincus PA, de Gennes P-G. Europhys Lett 1995;32:391.
[12] Samus MA, Rossi G. Macromolecules 1996;29:2275.
[13] Astarita G, Sarti G-C. Polymer Engng Sci 1978;18:388.
[14] Govindjee S, Simo JC. J Mech Phys Solids 1993;41:863.
[15] Brown HR, Argon AS, Cohen RE, Gebizlioglu OS, Kramer EJ. Macromolecules 1989;22:1002.
[16] Argon AS, Cohen RE, Gebizlioglu OS, Brown HR, Kramer EJ. Macromolecules 1990;23:3975.
[17] Brown HR. J Polymer Sci B 1989;27:1273.
[18] Nealey PF, Cohen RE, Argon AS. Polymer 1995;36:3687.
[19] Gebizlioglu OS, Beckham HW, Argon AS, Cohen RE, Brown HR. Macromolecules 1990;23:3968.
[20] Guggenheim EA. Thermodynamics: an advanced treatment for chemists and physicists. Amsterdam: North-Holland, 1950.
[21] Peterlin A. J Polymer Sci B 1965;3:1083.
[22] Argon AS. Phil Mag 1973;28:839.
[23] McClintock FA, Argon AS. Mechanical behavior of materials ch. 7. Reading, MA: Addison-Wesley, 1966.
[24] Kirchheim R. J Polymer Sci 1993;31:1373.
[25] Argon AS. In: Cahn RW, Haasen P, Kramer EJ, editors. Materials science and technology, vol. 6 (Mughrabi H, editor). Berlin: VCH Publishers, 1993:461.
[26] Argon AS, Bessonov MI. Phil Mag 1977;35:917.
[27] Argon AS. J Appl Polymer Sci 1999;72:13.
[28] Crank J. J Polymer Sci 1953;11:151.